Comparing the Structures and Photophysical Properties of Two Charge Transfer Co-crystals

Ali Abou Taka,[a] Joseph E. Reynolds III,[a] Neil C. Cole-Filipiak,[a] Mohana Shivanna,[a] Christine J. Yu,[b] Patrick Feng,[a] Mark D. Allendorf,[a] Krupa Ramasesha,[a] Vitalie Stavila,[a] and Laura M. McCaslin[a*]

In the search for molecular materials for next-generation optoelectronic devices, organic co-crystals have emerged as a promising class of semiconductors for their unique photophysical properties. This paper presents a joint experimental-theoretical study of ground and excited state charge transfer (CT) interactions in two CT co-crystals. Reported herein is a novel CT co-crystal Npe:TCNQ, formed from 4-(1-naphthylvinyl) pyridine (Npe) and 7,7,8,8-tetracyanoquinodimethane (TCNQ) molecules via molecular self-assembly. The electronic structure and photophysical properties of Npe:TCNQ are compared with those of the co-crystal composed of Npe and 1,2,4,5-tetracyanobenzene (TCNB) molecules, Npe:TCNB, reported here with a higher-symmetry (monoclinic) crystal structure than previously published. Npe:TCNB and Npe:TCNQ dimer clusters are used as theoretical model systems for the co-crystals and their electronic structure is compared to that of the extended solids via periodic boundary conditions density functional theory (PBC DFT). UV-Vis absorption spectra of the dimers are computed with time-dependent density functional theory (TD-DFT) and compared to experimental UV-Vis diffuse reflectance spectra. Both Npe:TCNB and Npe:TCNQ are found to exhibit neutral character in the S_0 state and ionic character in the S_1 state. The degree of CT in the S_0 state of Npe:TCNB is found to be slightly smaller than that of Npe:TCNQ, as predicted from differences in electron affinities of the acceptors. Furthermore, the degree of CT in the S_1 state of Npe:TCNB is found to be slightly higher than that of Npe:TCNQ, aligning with predictions employing a recently developed orbital similarity metric.

1. Introduction

In the search for semiconducting materials with tailored optoelectronic properties, organic co-crystals have emerged as particularly promising materials for integrated photonics, photovoltaic devices, and organic LEDs.[1-14] Co-crystals are crystalline, single-phase materials composed of two or more molecular compounds that interact noncovalently.[3] One class of these, charge transfer (CT) co-crystals, can be defined by CT interactions between molecular subunits of electron donor and acceptor molecules.[3] Organic CT co-crystals are particularly interesting for the development of optoelectronic devices, exhibiting behaviors such as ambipolar charge transport,[3,5,6] tunable emission,[7-9] and room temperature ferroelectricity.[2,10]

In the vast space of molecular complexity, finding combinations of donors and acceptors that produce co-crystals with optimal properties has inspired significant

[a]*Sandia National Laboratories, Livermore, California 94550, USA*
[b]*Department of Chemistry, Northwestern University, Evanston, Illinois 60208, USA*

**Correspondence should be directed to lmmccas@sandia.gov*
†*Electronic Supplementary Information (ESI) available*

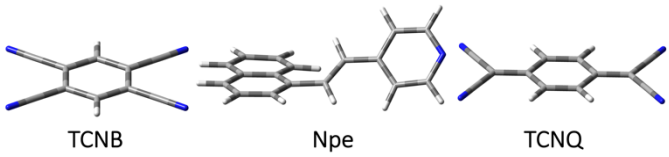

Figure 1: Structures of TCNB, Npe, and TCNQ

interest. Researchers use the principles of rational design to identify structure-function relationships and correlate properties of individual molecules to the properties of bulk materials.[3,11-14] Modern approaches to exploring chemical space have also emerged, such as high-throughput screening and machine learning.[15-19] These methods screen combinations of donor and acceptor molecules to predict materials' bulk physical properties from molecular metrics such as geometric and energetic parameters.[20] Machine learning and high-throughput screening approaches are continually improving via inclusion of new structure-function relationships, driving a need for fundamental studies that identify such relationships through crystallographic structure determination, spectroscopic characterization, and electronic structure characterization.

A recent paper from our group has identified a novel *orbital structure*-function relationship in donor-acceptor (D-A) materials, enabling predictions of the degree of S_1 CT using ground state orbital analysis alone.[21] For integration of such relationships into high-throughput screening procedures, metrics that quantify these relationships must be tested on new chemical systems where high-quality crystallographic and spectroscopic data are available. To this aim, we present a comparative study of the crystallographic structure, spectroscopy, and electronic structure of two D-A co-crystals: 4-(1-naphthylvinyl)pyridine (Npe) co-crystalized with 1,2,4,5-tetracyanobenzene (TCNB) and Npe co-crystalized with 1,2,4,5-tetracyanoquinodimethane (TCNQ), shown in Figure 1. We report a revised crystallographic study of Npe:TCNB, in which we find a monoclinic crystal structure, in contrast to the previously reported triclinic structure.[22] A crystal structure of the second system studied here, Npe:TCNQ, has not been reported to date; we thus present the first studies of the structure and photophysical properties of Npe:TCNQ. Theoretically, the S_0 optimized geometries of the D-A dimer models are computed using density functional theory (DFT) and compared to calculations of the extended solids via periodic boundary conditions (PBC) DFT to assess the role of the extended crystal in constraining molecular geometries of the D-A subunits. Comparisons of the experimental vs. theoretical UV-Vis spectra enable benchmarking theoretical cluster models against the experimentally studied extended solids. We report the degree of CT in the ground (S_0) and first electronically excited singlet state (S_1) of our theoretical dimer models to compare between the two co-crystal systems. Furthermore, we rationalize the degree of S_1 CT by computing the orbital similarity between isolated and D-A complexes, using our recently developed metric.[21]

2. Methods Section

2.1 Computational Methods

2.1.1 Methodology

A variety of DFT methods and basis sets were benchmarked and used to identify possible minimum energy structures along the neutral Npe:TCNB and Npe:TCNQ dimer surfaces, with additional information given in ESI Tables S1-S2. Geometry optimizations and relative energies were computed and compared using functionals ωB97X-D, B3LYP, B3LYP-D3, CAM-B3LYP, CAM-B3LYP-D3, and M06-2X and basis sets 6-31G(d,p), 6-31+G(d,p), and 6-311+G(d,p), resulting in 18 combinations of functional and basis set.[23–30] Here, a D3 suffix on the functional name refers to the Grimme D3 dispersion correction, needed for the calculation of non-covalent bonding interactions.[30] We find that CAM-B3LYP-D3/6-31+G(d,p) calculations of the dimer clusters best reproduce the geometries found in the experimental crystal structures and UV-Vis spectra without the need for any long-range parameter tuning. Geometry optimization calculations were also performed with periodic boundary conditions (PBC) DFT using the hybrid functional HSE06 and 6-31G(d,p) basis using crystallographic information file (CIF) geometries from the experimental crystal structure as initial guesses.[27-29,31] Hybrid functionals such as HSE06 combine semi local exchange and non-local Hartree-Fock exchange, which yields improved band gaps, excitation energies, and thermochemical properties over pure functionals (see Ref. 32 and references within). Structures were obtained by optimizing all coordinates and unit cell lengths using an energy convergence criterion of 10^{-5}. The number of k points used for Npe:TCNB is 28 and for Npe:TCNQ, 36. Direct band gaps are reported using these PBC DFT parameters. Excited state calculations were carried out using CAM-B3LYP-D3/6-31+G(d,p) within the linear response time–dependent DFT (TDDFT) formalism, with additional details given in ESI, Tables S3-S12 and Figures S14-23.[33-35] Natural bond orbital (NBO) population analyses[36] were performed to quantify the amount of CT in the ground state of the complexes, while transition density matrix analysis was used to calculate the degree of CT in the S_1 excited states using Theodore.[37] Excited state analysis was facilitated by Martin's Natural Transition Orbital (NTO) model.[38]

All calculations described in 2.1.1 were carried out using the GAUSSIAN suite of electronic structure programs, G16.[39] Stability was tested on all converged Kohn–Sham determinants.[40] Stationary points were verified as minima using harmonic frequency analysis, employing analytical second–derivative calculations.[41] All relative energies of structures are zero-point energy corrected, employing the harmonic approximation for frequency analysis. See ESI Tables S1-S2 and ESI Section 2.4 for more details.

Calculations of the orbital similarity are performed as suggested in our previous paper.[21] Orbital similarity is computed between donor HOMO and D-A dimer HOMO, as well as acceptor LUMO and D-A dimer LUMO, where values of orbital similarity range between 0 (no similarity) and 1 (same orbital). Donor and acceptor geometries are taken to be the geometries they assume in the optimized D-A dimer complex (i.e. donor and acceptor geometries are not geometric minima of the isolated molecules), allowing for the simplification that the overlap matrix of atomic basis functions between donor and D-A complex (as well as acceptor and D-A complex) is equivalent to the self-overlap of atomic basis functions, reported in the output of our electronic structure calculations.[21]

2.2 Experimental Methods

2.2.1 General Comments

All co-crystals were synthesized in ambient conditions. 1,2,4,5-tetracyanoquinodimethane (TCNQ) was purchased from Acros Chemical and used as received. 1,2,4,5-tetracyanobenzene (TCNB) and 4-(1-naphthylvinyl)pyridine (Npe) were purchased from TCI America and used as received. All organic solvents were purchased from Sigma-Aldrich and used as received.

2.2.2 General Instrumentation

Powder X-ray Diffraction (PXRD): Patterns for the bulk powders were collected with a Panalytical Empyrean Diffractometer system equipped with a PIXcel3D detector using CuKα radiation using samples loaded in glass capillaries (Charles Supper, Inc.) and sealed with vacuum grease. See Figures 5, 7.

Single Crystal X-Ray Crystallography (SCXRD): Suitable crystals were mounted on a thin glass fiber using perfluoropolyether oil, which was frozen in situ by a nitrogen gas cryostream flow. Data collection was performed on a Rigaku Super Nova diffractometer equipped with an AtlasS2 CCD, and Oxford 700 low-temperature attachment, using CuKα (λ = 1.54184). Using Olex2, structures were solved with the SHELX structure solution program using Direct Methods and refined with the SHELXL refinement package using least squares minimization. See additional details in ESI, Figures S1-S9 and ESI Section 3.

Fourier Transform Infrared (FTIR): Spectra were obtained with an Agilent Cary-630 spectrometer, with an attenuated total reflectance module containing a diamond crystal. See additional info in ESI, Figures S10-S11.

Elemental Microanalyses: Elemental microanalyses were performed by Galbraith Laboratories, Inc. (Knoxville, TN).

Photoluminescence (PL) Spectroscopy: Photoluminescence spectra were collected using an Edinburgh Instruments FLS1000 fluorimeter equipped with a 450 W Xenon arc lamp for steady-state measurements and a 375 nm picosecond pulsed light emitting diode for time-resolved measurements. Single-grating Czerny-Turner excitation and emission monochromators were used along with a cooled PMT-900 photomultiplier detector that covers a range of 185-900 nm. Absorption spectra were collected between 300-540 nm monitoring the emission at a wavelength of 550 nm.

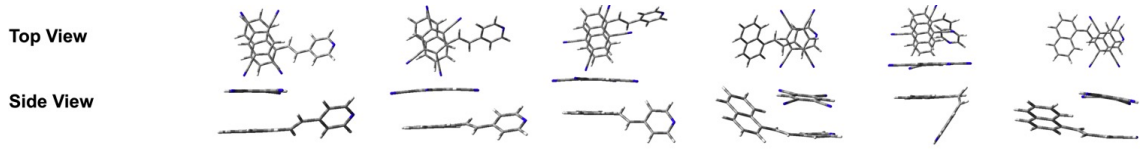

		a	b	c	d	e	f
$Energy_{rel}$ (eV)		0.000	0.009	0.062	0.107	0.111	0.179
Degree of CT (e)	S_0	0.02	0.02	0.02	0.01	0.02	0.01
	S_1	0.97	0.97	0.97	0.98	0.96	0.98
Osc. Strengths (au)		0.021	0.003	0.009	0.016	0.023	0.002

Figure 2: Optimized geometries of Npe:TCNB found with CAM-B3LYP-D3/6-31+G(d,p). Energies (eV) are reported relative to the lowest-energy structure (a) and include zero-point corrections. The calculated degree of CT is also reported for S_0 and S_1 with the associated oscillator strength for S_1 excited states.

Emission spectra were collected between 424-740 nm with an excitation wavelength of 375 nm. See Figure 5b-c.

2.2.3 Synthesis of Npe:TCNB co-crystals

Npe:TCNB co-crystals were synthesized by dissolution of 0.5 mmol TCNB and 0.5 mmol Npe in a 20 mL vial with 6 mL of a 1:1 DMF:MeCN solvent. Once fully dissolved, the yellow solution was allowed to slowly evaporate forming broad needle-like crystals. A bulk powder form of the Npe:TCNB co-crystals can be formed by mixing two separate TCNB and Npe solutions in pure MeCN.

2.2.4 Synthesis of Npe:TCNQ co-crystals

Npe:TCNQ co-crystals were synthesized by dissolution; 0.15 mmol of Npe and 0.1 mmol of TCNQ were combined in a 7 mL vial with 4 mL of MeCN and heated/boiled until all solids were dissolved, resulting in a dark green solution that forms small blue-like plates as it slowly cools to room-temperature overnight. (Note: the crystallographic ratio is the opposite of the synthesis conditions). Further purification and isolation were achieved by washing with cold MeCN. Elemental Analysis of 2Npe:3TCNQ co-crystal: C_{17} H_{13} N,1.5(C_{12} H_4 N_4). Calculated: C 78.20, H 3.56, N 18.24; Found: C 77.30, H 3.22, N 17.84.

2.2.5 Diffuse Reflectance Spectra

UV-Vis and near-IR spectra of solid Npe, TCNB, TCNQ, Npe:TCNB, and Npe:TCNQ were acquired in diffuse reflectance mode using a Perkin-Elmer Lambda 1050+ spectrophotometer. Samples were finely ground and mixed with MgO powder (~40 μm particle size) to make ~1 wt.% mixtures. Sample mixtures were then pressed against a CaF_2 window mounted onto the side of a 100 mm integrating sphere.

2.2.6 Band Gap Determination

To estimate the optical band gap of each co-crystal, the diffuse reflectance spectra shown in Figures 6c, 8c were first transformed using the Kubelka-Munk transformation.[42] The resulting *F(R)* spectra were treated as a pseudo-absorption function, assuming the scattering coefficient is constant for small spectral windows near the onset of the lowest energy feature. In this approximation, the linear portion

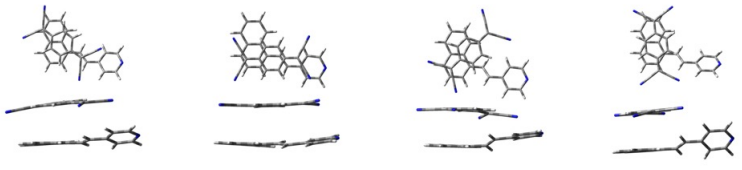

		a	b	c	d
Top View					
Side View					
$Energy_{rel}$ (eV)		0.000	0.010	0.026	0.029
Degree of CT (e)	S_0	0.04	0.07	0.04	0.01
	S_1	0.95	0.92	0.95	0.97
Osc. Strengths (au)		0.030	0.065	0.026	0.002

Figure 3: Optimized geometries of Npe:TCNQ found with CAM-B3LYP-D3/6-31+G(d,p). Energies (eV) are reported relative to the lowest-energy structure (a) and include zero-point corrections. The calculated degree of CT is also reported for S_0 and S_1 with the associated oscillator strength for S_1 excited states.

of plots of $F(R)^{1/\gamma}$ *vs*. photon energy was extrapolated to the x-axis to determine the optical band gap.[43] For direct band gap materials, such plots will appear linear for $\gamma = 1/2$ whereas indirect band gap materials will show good linearity for $\gamma = 2$. *F(R)* plots for both materials, along with linear extrapolations, are presented in ESI, Figures S12-S13. As none of these *F(R)* plots show obvious improvements in linearity, we report the direct band gap. Due to the vibronic structure observed in Npe:TCNQ, multiple linear fits were performed up to the lowest energy shoulder at ~862 nm.

	Npe-Npe:TCNB (HOMO)	TCNB-Npe:TCNB (LUMO)	Npe-Npe:TCNQ (HOMO)	TCNQ-Npe:TCNQ (LUMO)
Orbital Similarity	0.99	0.99	0.98	0.98
Average Similarity	0.99		0.98	

Table 1:Values of the orbital similarity are reported for each system along with the average similarity value.

3. Results and Discussion

In high-throughput screening procedures, dimer cluster geometries are optimized to determine a low-energy conformer for which properties such as orbital energies and vibrational frequencies are calculated. Detailed benchmarking of (1) the level of theory/basis set, and (2) comparison of theoretical and experimental spectroscopic data is generally not performed in screening procedures due to computational expense and difficulty. We perform these detailed benchmarking and comparison studies here to develop and improve databases of crystallographic, spectroscopic, and electronic structure data.

In this section we compare D-A co-crystal systems with commonly used donor and acceptor molecules previously employed in co-crystal materials with unique optical properties. These two co-crystal systems have the same donor molecule, Npe, and structurally similar acceptors, TCNB and TCNQ. The first acceptor, TCNB, has been used in the synthesis of co-crystals for applications in developing waveguides and photoswitches.[22,44,45] The second acceptor, TCNQ, is one of the most widely studied acceptor species due to its high electron affinity (EA). [6,46-49] TCNQ-based co-crystals are known for strong CT character and some exhibit room temperature ambipolar charge transport.[6,46-49] While Npe:TCNB co-crystals have recently been of interest in the development of waveguides for integrated photonics,[22] to the authors' knowledge, Npe:TCNQ co-crystals have not been reported to date.

3.1 Comparing Orbital Overlap and Charge Transfer of Npe:TCNB and Npe:TCNQ

We performed scans of the potential energy surfaces (PES) of Npe:TCNB and Npe:TCNQ using CAM-B3LYP-D3/6-31+G(d,p) with additional details in Section 2.1.1. Figures 2 and 3 show the minimum geometries identified for each system. To best model the conditions of a high-throughput screening procedure, our tests of the recently developed orbital similarity metric are performed on the lowest-energy isomer for each system.[21] Additional benchmarking to confirm the chosen models is described in Sections 3.2-3.3.

Figure 4 presents the HOMO and LUMO isosurfaces and orbital energies of Npe, TCNB, TCNQ, Npe:TCNB, and Npe:TCNQ. One of the most striking features of the orbital isosurfaces is the similarity of the Npe:acceptor complexes' HOMO and Npe HOMO isosurfaces, as well as those of the Npe:acceptor complexes' LUMO and acceptor LUMO. Because a large degree of CT is observed in the S_1 states (HOMO→LUMO) of each complex, we look for correlations between the degree of similarity between isolated vs. complexed orbitals and the degree of S_1 CT, using our recently developed method,[21] shown in Table 1. In the case of Npe:TCNB, we find an overlap of 0.99 between the Npe HOMO and Npe:TCNB HOMO (Npe-Npe:TCNB) and an overlap of 0.99 between the TCNB LUMO and Npe:TCNB LUMO (TCNB-Npe:TCNB). In the case of Npe:TCNQ, overlap values are calculated to be 0.98 between the Npe HOMO and Npe:TCNQ HOMO (Npe-Npe:TCNQ) and 0.98 between the TCNQ LUMO and Npe:TCNQ LUMO (TCNQ-Npe:TCNQ). Our explicit calculations of the degree of CT in S_1 using TDM analysis (See Figures 2 & 3) reveal a high degree of CT in both complexes, with 0.97e in the S_1 state of Npe:TCNB and 0.95e in the S_1 state of Npe:TCNQ. Comparing HOMO overlap between Npe-Npe:TCNB (0.99) and Npe-Npe:TCNQ (0.98), Npe-Npe:TCNB exhibits a 1% higher overlap than that of Npe-Npe:TCNQ. The LUMO overlap between TCNB-Npe:TCNB (0.99) is also 1% higher than that of TCNQ-Npe:TCNQ LUMO (0.98). Taking the average of the HOMO and LUMO values for each complex, as shown in Table 1, we see that the average orbital similarity for Npe:TCNB is 0.99 vs. 0.98 for Npe:TCNQ, revealing that Npe:TCNB has a slightly higher orbital similarity (1%) than Npe:TCNQ, as expected from the slightly higher degree of S_1 CT in Npe:TCNB (0.97e vs. 0.95e in Npe:TCNQ). While these differences in orbital similarity between Npe:TCNB and Npe:TCNQ are quite small, we find that the degree of orbital similarity is very high for both complexes, as expected from the large degree of S_1 CT in both systems.

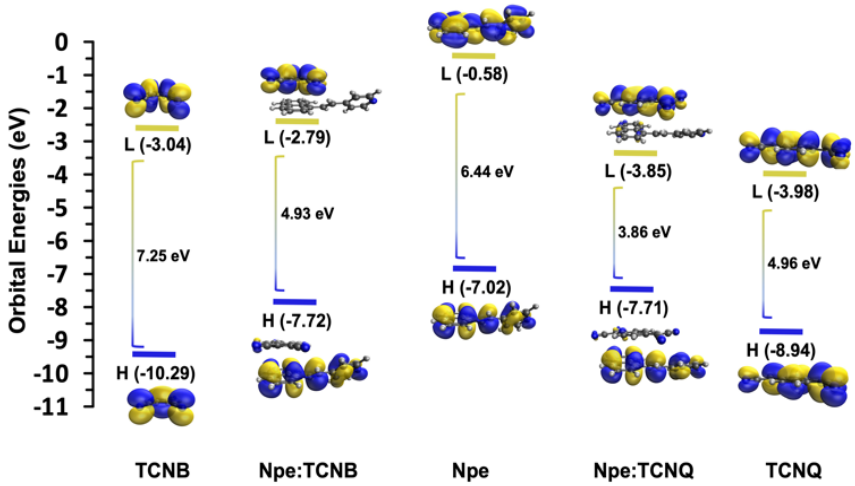

Figure 4: The molecular orbital energy level diagram for Npe:TCNQ and Npe:TCNB complexes with their isolated molecules. Orbital energy gaps are also shown. Orbitals are plotted with isovalue of 0.05 Å^{-3}.

We now turn to comparing orbital energies using well-established techniques. Prior studies have used the metric E_{HOMO}^{donor}-$E_{LUMO}^{acceptor}$ to identify the degree of CT in the ground state, with larger values of E_{HOMO}^{donor}-$E_{LUMO}^{acceptor}$ representing higher values of S_0 CT.[20] The energy difference between isolated Npe HOMO and TCNB LUMO (E_{HOMO}^{Npe}-E_{LUMO}^{TCNB}) is (-7.02 eV) – (-3.04 eV) = -3.98 eV. In the Npe and TCNQ orbital analysis, we observe an E_{HOMO}^{Npe}-E_{LUMO}^{TCNQ} difference of –(-7.02 eV) – (-3.98 eV) = -3.04 eV. Comparing the E_{HOMO}^{Npe}-$E_{LUMO}^{acceptor}$ values between the two systems, we observe that E_{HOMO}^{Npe}-E_{LUMO}^{TCNQ} = –3.04 eV is higher than E_{HOMO}^{Npe}-E_{LUMO}^{TCNB} = –3.98 eV, indicating a larger degree of S_0 CT.

We can also compare the orbital energies between Npe:TCNB and Npe:TCNQ using an analysis based on Koopman's theorem to assess the degree of S_0 CT, estimating that the EA is approximately equal to the negative of the LUMO energy. This gives an EA^{TCNB} of 3.04 eV vs. an EA^{TCNQ} of 3.98 eV. Comparing the estimations of EA to calculations of ground state CT using an NBO analysis, we observe that Npe:TCNB exhibits smaller degree of CT, 0.02e, vs. 0.04e in Npe:TCNQ, as expected from TCNB's smaller EA.

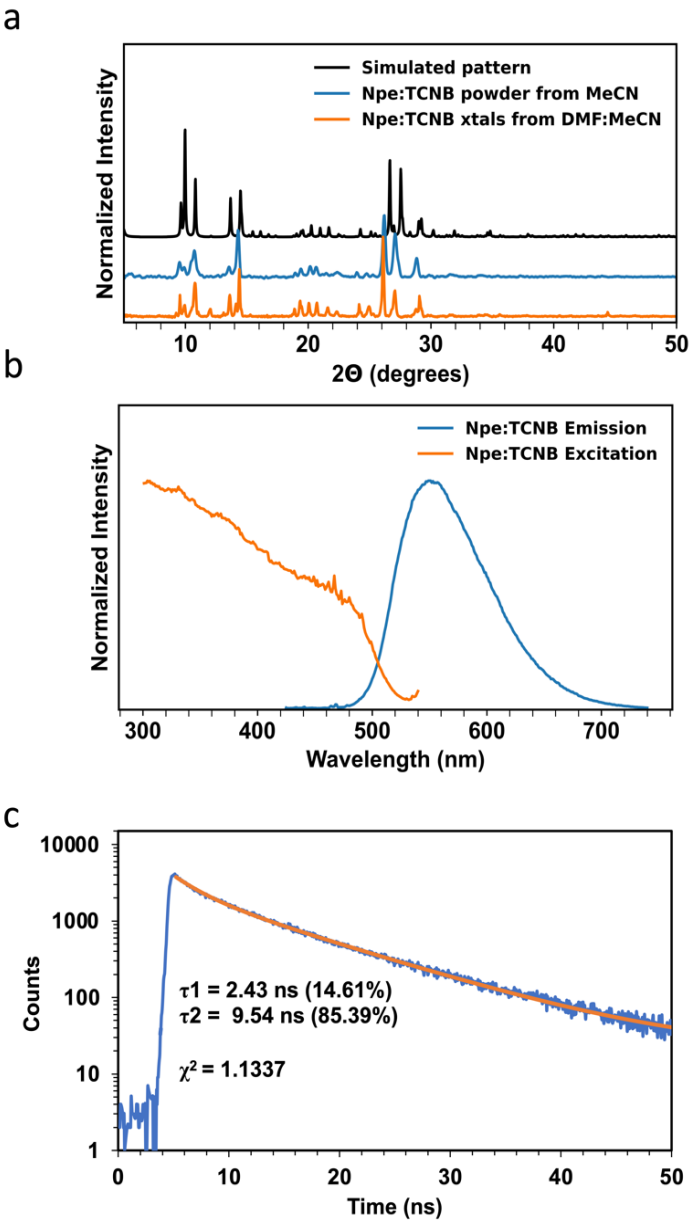

Figure 5: a) Powder X-ray patterns of Npe:TCNQ obtained from simulation of the crystal structure (top trace), MeCN (middle trace), and by DMF/MeCN (bottom trace). B) The absorption and PL spectra of Npe:TCNB co-crystals on a glass substrate at 298 K. c) The PL decay profile (with fitting curve).

3.2 Structural and Electronic Characterization of Npe:TCNB

We now turn to detailed benchmarking of our model systems against experimental crystal structures and spectroscopic data to confirm our choice of the lowest-energy D-A dimer as a sufficient model for these crystalline materials. As briefly described in 3.1, we performed scans of the S_0 PES of the Npe:TCNB molecular cluster (MC) and identified six

structures as candidate dimer models of the extended co-crystals, shown in Figure 2. A previous study identified two low-energy minimum geometries of the Npe:TCNB dimer.[22] In the six conformers identified here, two agree with the previously reported geometries by Zhu et al., including the lowest-energy isomer, a. We find that multiple minima exist upon rotation of TCNB with respect to the naphthalene of Npe, resulting in our identification of two low-energy structures that differ by 0.009 eV (b) and 0.062 eV (c) from the lowest-energy structure. We also identify a structure at 0.107 eV for which TCNB is localized to the pyridine of the Npe (d). The highest energy structure (0.179 eV, f) found in this study is structurally similar to the higher energy structure determined by Zhu et al., differing only by a slight rotation of the naphthalene ring.[22] Finally, a folded structure was located at a relative energy of 0.111 eV (e). In this structure, the Npe molecule is folded in a V-shape and TNCB is positioned on top of the naphthalene moiety.

To compare our model structures to experimental values, Npe:TCNB crystals were synthesized and spectroscopically characterized. Single crystals of Npe:TCNB were grown by slow evaporation of a 1:1 molar ratio of TCNB and Npe dissolved in a 1:1 (vol.) DMF/MeCN mixture, resulting in yellow blade-like crystals suitable for single-crystal X-ray diffraction (SCXRD). Analysis by SCXRD determined that the Npe:TCNB co-crystal, in contrast to the previously reported triclinic structure,[22] crystallizes with a 1:1 ratio of TCNB to Npe in the monoclinic space group P21/c with a = 6.73, b = 36.66, and c = 9.51 Å(β = 106◦). Although the single-crystal XRD measurement was performed at 100 K, there is still a large amount of disorder around the pyridine moiety of Npe, which appears to be "rocking" and generating an additional conformation of the pyridine ring that is >45◦ out of the plane with respect to the other occupied pyridine site. The expanded structure reveals that there is a π – π stacking interaction between the naphthalene moiety of the Npe and the benzene ring of the TCNB molecule with a distance of 3.375 Å. The pyridine of Npe interacts with other Npe-pyridines in adjacent layers with a centroid-centroid distance of 3.9 – 4.9 Å, Figure S4. The crystal structure shows no evidence of interaction between the Npe pyridine moiety and TCNB. Further details on the crystal structure data are given in ESI Section 3.

Steady-state and time-resolved photoluminescence measurements were collected on Npe:TCNB co-crystals to further probe the interactions between the Npe and TCNB moieties, as shown in Figures 5b and 5c. The emission spectra show a single peak centered near 550 nm, which is red shifted ~100 nm from that of Npe itself. This shift is associated with CT interactions between Npe and TCNB.[50] The observed fluorescence decay for Npe:TCNB follows a bi-exponential decay with decay components of 2.43 ns (14.6%) and 9.54 ns (85.4%). These values differ from that of pure Npe (1.57 ns) and reflect appreciable electronic interactions in the excited state between the two co-crystal components.

The centroid-centroid distances between Npe and TCNB in the six isomers shown in Figure 2 agree with the experimentally observed distances, ranging between 3.3 and 3.5 Å. The values quantifying degree of CT are very consistent for all isomers in the S_0 and S_1 states, varying between 0.01e and 0.02e in S_0 and between 0.96e and 0.98e in S_1, as shown in Figure 2. In all isomers found, the S_1

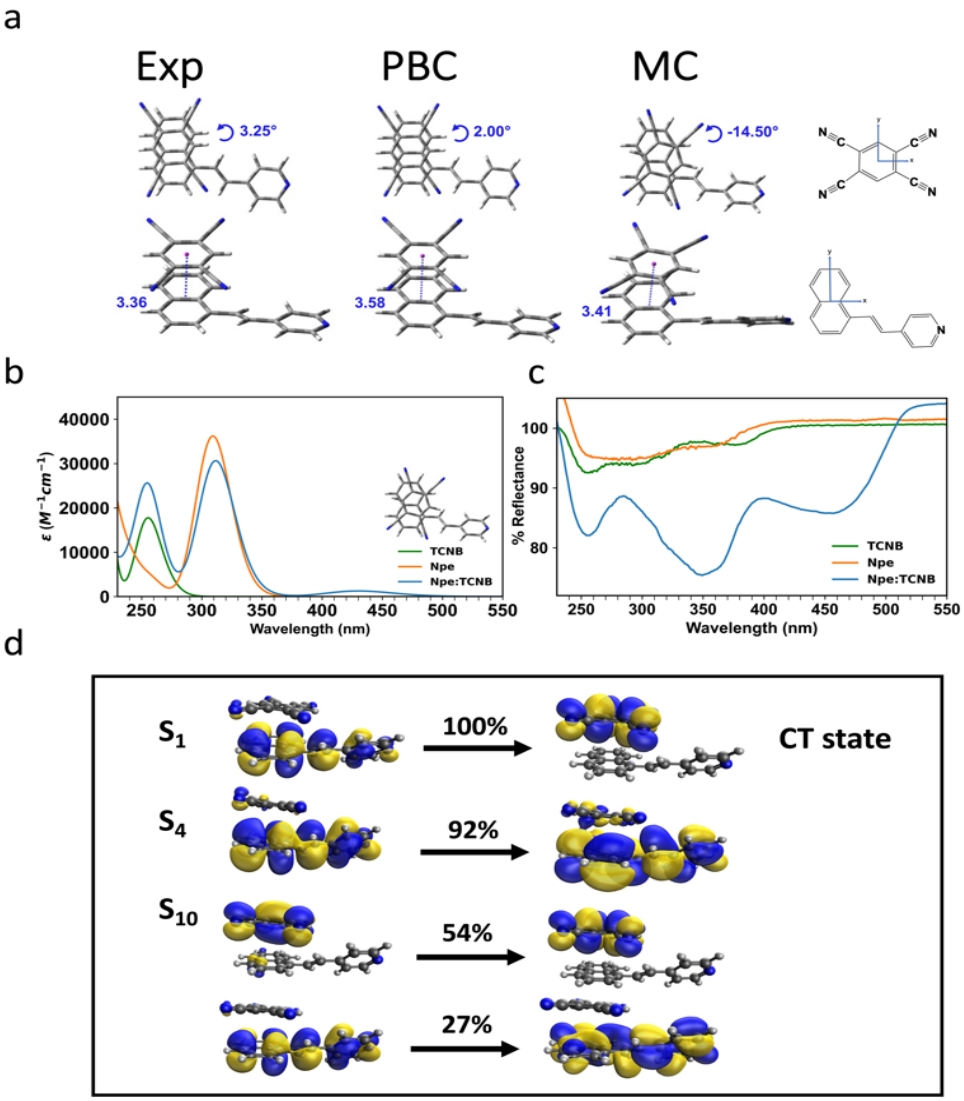

Figure 6: a) Geometries of Npe:TCNB from the experimental crystal structure (Exp), periodic boundary condition (PBC) DFT, and molecular cluster (MC) calculations (centroid-centroid distances are indicated with dotted line in Å). b) The simulated absorption spectra of Npe, TCNB, and Npe:TCNB in the MC. c) Diffuse reflectance spectra of ~1 wt.% mixtures of Npe, TCNB, and Npe:TCNB. d) Orbital contributions of strong electronic transitions and their associated weights.

state is a CT state characterized by the HOMO to LUMO transition. The computed oscillator strengths of these transitions, however, are quite different. Isomers a, d, and e exhibit S_1 oscillator strengths with values of 0.021, 0.016, and 0.023 a.u., respectively, higher than the other conformers where the S_1 state oscillator strength values range from 0.002 to 0.009 a.u. Of these, structure a (the lowest-energy isomer) is far closer geometrically to the experimental crystal structure than d or e, allowing structure a to emerge as the best model for Npe:TCNB, as predicted from energetic arguments alone in Section 3.1.

PBC DFT calculations were carried out to study the effects of the extended solid on the geometry of the unit cell and found to be in agreement with the both the experimental crystal structure and MC model, shown in Figure 6a. Due to the significant computational expense of PBC DFT calculations, we can only compute ground state geometries and energies. We thus focus our comparison between ground state PBC DFT and MC calculations. Two main structural differences are observed in the comparison between the PBC DFT structure and its MC counterpart. First is the alignment of the TCNB molecule relative to Npe. The MC structure exhibits a -15.50° rotation of the TNCB, while the PBC DFT structure exhibits a 2.0° rotation, and experimental crystal structure a 3.25° rotation. Another key difference is the planarity of Npe observed in the structures, calculated as the dihedral between the pyridine and naphthalene moieties. This dihedral angle is 2.8° in the PBC DFT structure and 13.3° in the MC structure, compared to the 2.0° in the experimental crystal structure. While we see larger differences between the MC geometry and experimental structure compared to the PBC DFT geometry, these geometric differences are relatively minor, with MC structures exhibiting the qualitative features of the crystal structure. Some geometric differences between PBC DFT and MC structures are to be expected, as the crystal structure constrains the structures of the D-A pairs. We thus turn to assess the importance of these structural differences via comparisons of the experimental UV-Vis spectra and theoretically predicted UV-Vis spectra of the dimer cluster.

While we have strong structural and energetic arguments for our choice of the optimal MC model of Npe:TCNB, we must compare the computed UV-Vis absorption spectra to the experimental UV-Vis diffuse reflectance spectra, shown in Figure 6 b-c. Here we compare dips in the experimental reflectance spectra to calculated absorption peaks. The exact % R peak shapes will not be examined closely, as features such as >100% R values shown at low wavelength are likely due to fluorescence emission and outside the scope of this discussion. The calculated S_1 state at 430 nm with oscillator strength f = 0.021 a.u. is characterized by a HOMO→LUMO transition, originating from intermolecular CT from Npe to TCNB, as shown in Figure 6d. This transition corresponds to the experimentally observed dip around 450 nm (Figure 6 b-c). The peak computed at 310 nm corresponds to the S_4 excited state, f =0.478, seen experimentally at 350 nm. In contrast to the CT character of the S_1 state, the S_4 state exhibits local excitation within Npe, as seen in Figure 6d. The theoretical S_{10} peak, f =0.356, computed at 250 nm (in excellent agreement with the experimental dip at 250 nm), is characterized by two orbital transitions, both with locally excited character, shown in Figure 6d. The good agreement between the simulated spectrum of the cluster model and the experimental diffuse reflectance spectrum of the crystals supports our choice of the lowest-energy cluster model and aids in the characterization of the electronic structure involved in photon-induced CT.

The UV-Vis diffuse reflectance spectra were analyzed to determine the band gap of Npe:TCNB crystals, as described in Section 2.2.6. A direct band gap is determined as 2.45 eV. Our PBC DFT calculations determine the direct band gap to be 2.03 eV. The difficulties with which PBC DFT computes accurate band gaps are well documented, though hybrid functionals such as the one used in this study

balance local and non-local exchange, resulting in computed band gaps that compare favorably with experimental values (see Ref. 32 and references within). We thus find reasonably good agreement between the PBC DFT and experimentally derived direct band gaps.

3.3 Structural and Electronic Characterization of Npe:TCNQ

We now turn to studying the electronic structure, crystal structure, and UV-Vis spectra of Npe:TCNQ. We performed scans of the PES of the Npe:TCNQ dimer to identify structures of the model cluster that best reproduce the crystal structure. Figure 3 shows the optimized minimum-energy structures located on the Npe:TCNQ dimer PES. Four low-energy dimer structures were identified with a 0.029 eV energy gap between the lowest and the highest energy structure. The four conformers differ from each other by the rotation of the TCNQ above the phenyl rings with significant rotations of the pyridine ring in conformers b and c, labeled in Figure 3. An intermolecular distance of 3.4 Å is found in all structures except b, with a shorter inter-ring distance of 3.2 Å. This shorter distance can be explained by the alignment of the TCNQ molecule above the Npe molecule that results in strong hydrogen bonding between the N atoms of the TCNQ and the H atoms of the Npe pyridine ring.

To ensure that the lowest-energy conformer of Npe:TCNQ is the closest in structure to a D-A subunit in the extended solid, crystals of Npe:TCNQ were synthesized and characterized. Single crystals of the Npe:TCNQ co-crystal were grown by slowly cooling a warm solution of TCNQ and Npe dissolved in MeCN at 330 K. This resulted in precipitation of large dark blue prismatic crystals. Analysis by SCXRD (Figure 7) determined that the Npe:TCNQ crystallizes with a 2:3 ratio in the triclinic space group P-1 with cell parameters of a = 9.88, b = 11.81, c = 12.31 Å, α = 93.8◦, β = 93.94◦, and γ = 111.87◦. The crystal structure reveals layers of TCNQ and Npe alternating in pairs similar to that of the Npe:TCNB co-crystal as shown in Figures S5-S9 of the ESI. The stacking of the layers displays a pair of TCNQ molecules lining up above a single Npe molecule from an adjacent layer. The close proximity of the layers enables a π − π stacking interaction between the naphthalene moiety of the Npe with one TCNQ (3.730 Å) and an interaction with a second TCNQ and the pyridine moiety of the Npe (3.841 Å). Despite the close interactions between TCNQ and Npe within the same layer, the distance between the two interlayer Npe pyridine moieties is too large (4.847 Å) for substantial π – π interaction. Further details on the crystal structure data are given in ESI Section 3.

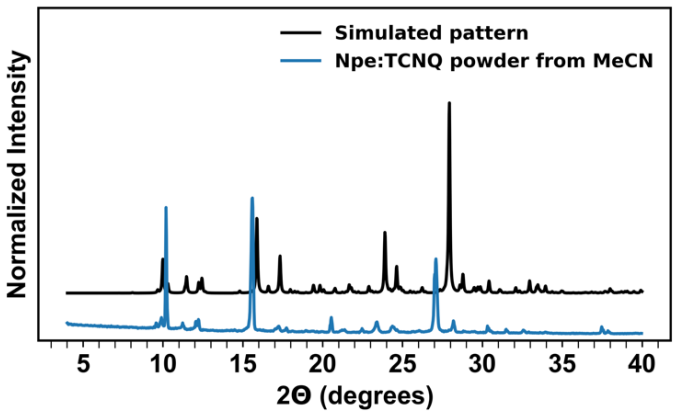

Figure 7: Powder X-ray patterns of Npe:TCNQ (bottom trace) and simulated from the crystal structure (top trace).

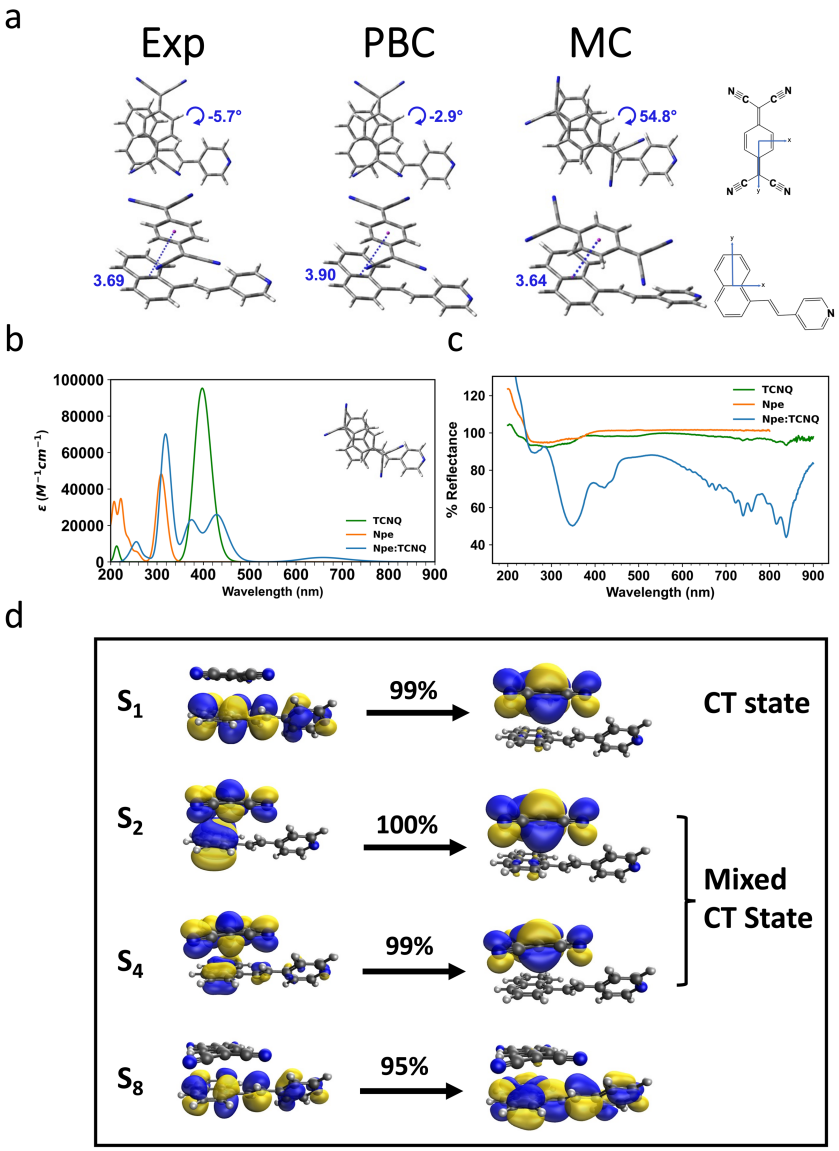

Figure 8: a) Geometries of Npe:TCNQ found with the experiment (Exp), periodic boundary condition (PBC) DFT, and molecular cluster (MC) calculations (centroid-centroid distances are indicated with dotted line in Å). b) The simulated absorption spectra of Npe, TCNQ, and Npe:TCNQ in the MC. c) Diffuse reflectance spectra of Npe, TCNQ, and Npe:TCNQ in MgO. d) Orbital contributions of strong electronic transitions and their associated weights.

Photoluminescence measurements were attempted for the Npe:TCNQ system, though no detectable fluorescence was observed. We attribute the fluorescence quenching to self-absorption effects.[51] Currently underway are studies of the UV pump, UV-Vis probe ultrafast transient absorption spectroscopy of Npe:TCNQ to reveal time-resolved luminescence data, which we will report in an upcoming paper.

We compare the experimental crystal structure of Npe:TCNQ to the dimer structures shown in Figure 3. Structures b and c exhibit significant rotation of TCNQ relative to Npe, differing substantially from the crystal structure's D-A subunit

geometry. In analysis of the degree of CT in the S_0 and S_1 states, we find that these quantities vary between conformers of Npe:TCNQ far more than in Npe:TCNB. In the S_0 state, CT values range from 0.01 to 0.07e, while in the S_1 state, CT values range from 0.92 to 0.97, exhibiting neutral character in the S_0 state and ionic character in the S_1 state, as seen in Npe:TCNB. We turn to the S_1 oscillator strength to assess our choice of the lowest-energy conformer a as our model. Indeed, we find that conformer a emerges as the optimal candidate, as its S_1 oscillator strength is sufficiently large (0.030 a.u. compared to 0.002 a.u. in structurally similar isomer d).

PBC DFT calculations were performed to quantify the effects of the extended solid on the structure of the D–A subunit in the crystal. Figure 8a shows that the PBC DFT calculated structure is in good agreement with the experimentally observed structure with a centroid-centroid distance difference of 0.21 Å between experiment and PBC DFT. The main differences between the PBC and MC structures are: 1) the degree of rotation of TCNQ with respect to Npe and 2) the centroid-centroid distances. There is a larger degree of rotation observed in the MC structure, 60.5° compared to the experimental crystal structure, whereas the rotation in the PBC structure differs from the experimental crystal structure by 2.8°, consistent with the findings in the case of Npe:TCNB. Although a higher degree of rotation is observed in the MC structure, the centroid-centroid distance exhibits smaller deviation from the experimental crystal structure, 0.05 Å, than the distance deviation between the PBC DFT structure and experiment, 0.21 Å. Due to the larger differences between MC and crystal structure, we turn to comparing the theoretical and experimental UV-Vis spectra to validate MC model.

The absorption spectra of our model Npe:TCNQ dimer were calculated, shown in Figure 8b. The simulated spectrum of Npe:TCNQ shows a peak at 660 nm, associated with the S_1 excited state. This state corresponds to CT from the Npe to the TCNQ with oscillator strength, f = 0.0299 a.u. and a HOMO→LUMO orbital transition, as shown in the orbital isosurfaces in Figure 8d. This peak is observed experimentally within the vibronic structure region between 600 and 900 nm. Two additional peaks in the calculated spectrum are located at 440 and 380 nm, associated with excited states S_2 and S_4, respectively. These two states have higher oscillator strengths, f = 0.310 a.u. and 0.280 a.u. for S_2 and S_4, respectively, with mixed character between locally excited and CT transitions, originating mainly from the TCNQ $\pi \rightarrow \pi*$ transition. These peaks likely correspond to the less intense dip observed in the experimental spectrum at 420 nm. A final strong peak at 320 nm originates from the S_8 excited state with strong oscillator strength, f = 0.860 a.u., aligning with the observed experimental dip at 340 nm. This excitation is characterized by the intramolecular Npe $\pi \rightarrow \pi*$ transition; see Figure 8d. Similar vibronic structure observed between 600 and 900 nm in other co-crystals has been attributed to formation of radical anion pairs of TCNQ and donor.[53-54] However, this assignment has recently come under scrutiny with evidence indicating that donor:TCNQ co-crystals can exhibit a small degree of CT in the S_0 state and a large degree of CT in the S_1 state, indicating formation of a radical anion pair only in the S_1 state.[55] To explain this, the authors refer to the foundational work of Mulliken on D–A pairs and the emergence of CT.[56] Mulliken's two-state system model describes a D–A pair as a linear

combination of neutral and ionic states, wherein systems with ground states that exhibit predominantly neutral character must necessarily exhibit predominant ionic character in an excited state due to orthogonality requirements. In our calculations of CT in the S_0 and S_1 states of Npe:TCNQ, we also find dominantly neutral character in S_0 and ionic character in S_1, supporting the assignment of Monezi et al.[55]

The UV-Vis diffuse reflectance spectra were analyzed to determine the band gap of Npe:TCNQ crystals, as described in Sections 2.2.6 and 3.2. A direct band gap is determined as 1.38 eV. Our PBC DFT calculations determine the direct band gap to be 0.79 eV. In the case of Npe:TCNQ, PBC DFT and experimental band gaps do not agree as nicely as in the case of Npe:TCNB, but still fall within typical deviations for hybrid functionals.[32]

4. Conclusions

In this work we test a recently developed method for correlating ground state orbital characteristics with degree of S_1 CT in CT co-crystals in the pursuit of uncovering *orbital structure*-function relationships. We quantify the orbital similarity between donor HOMO and D-A HOMO as well as acceptor LUMO and D-A LUMO to predict the degree of S1 CT in HOMO → LUMO dominated electronic transitions, finding that the degree of orbital similarity positively correlates with degree of CT in the S_1 state.

The availability of accurate crystal structures of CT co-crystal complexes is essential for developing chemical databases used by high-throughput screening methods for materials discovery. To this aim we report details of the syntheses and crystal structures of Npe:TCNB and Npe:TCNQ co-crystals. Our reinvestigation of the crystal structure of Npe:TCNB reveals a monoclinic structure, previously assigned as triclinic.[22] High-resolution crystal structures are necessary for benchmarking theoretical models and identifying structural effects of component molecules on crystal packing. Experimental UV-Vis diffuse reflectance spectra were measured to assess the peak positions and intensities of bright states of the co-crystals. Comparing relative intensities of these states to those calculated for theoretical molecular model systems plays an integral role in assessing the quality of our D-A dimer models. Furthermore, experimental UV-Vis diffuse reflectance spectra of Npe:TCNQ reveal vibronic structure in the 600-900 nm region, indicating strong photon-induced CT. NBO analysis of the ground state of our model clusters reveals that the degree of S_0 CT is slightly greater in Npe:TCNQ than in Npe:TCNB, as predicted from tests of the recently developed orbital similarity metric.[21] We find that differences in the S_0 and S_1 degree of CT in each system are quite small, with each system exhibiting dominantly neutral character in the S_0 state and ionic character in the S_1 state. The integrated experimental-theoretical methodology presented here for quantifying ground and excited state CT in CT co-crystals enables high-accuracy benchmarking of models for future discovery of novel co-crystals with desired optoelectronic properties.

Author Contributions

A.A.T. performed the calculations and analysis and co-wrote the manuscript. J.E.R. synthesized the crystals and aided in characterization. N.C.C-F. performed UV-Vis diffuse reflectance spectroscopy and provided insights into spectral assignments. M.S.

aided in characterization of the co-crystals. C.J.Y. aided in synthesizing and characterizing the co-crystals. P.F. aided in performing the photoluminescence experiments. M.A. provided insights on the connection of this work with the greater literature. K.R. aided in performing UV-Vis diffuse reflectance spectroscopy, provided insights into spectral assignments, and made connections with the literature. V.S. proposed study of the Npe:TCNQ, aided in synthesis of the crystals, aided in characterization of the crystals, and provided insights into connecting to the literature. L.M.M. aided in performing calculations and analysis of the orbital similarity and co-wrote the manuscript. All authors contributed to the interpretation of the results.

Conflicts of interest

There are no conflicts to declare.

Acknowledgements

The authors would like to thank Dr. Shinae Kim for her comments on the manuscript and Dr. Kevin Carter-Fenk for discussions on PBC DFT. This work is supported by the Laboratory Directed Research and Development program at Sandia National Laboratories. Sandia National Laboratories is a multi-mission laboratory managed and operated by National Technology & Engineering Solutions of Sandia, LLC (NTESS), a wholly owned subsidiary of Honeywell International Inc., for the U.S. Department of Energy's National Nuclear Security Administration (DOE/NNSA) under contract DE-NA0003525. This written work is authored by an employee of NTESS. The employee, not NTESS, owns the right, title and interest in and to the written work and is responsible for its contents. Any subjective views or opinions that might be expressed in the written work do not necessarily represent the views of the U.S. Government. The publisher acknowledges that the U.S. Government retains a non-exclusive, paid-up, irrevocable, world-wide license to publish or reproduce the published form of this written work or allow others to do so, for U.S. Government purposes. The DOE will provide public access to results of federally sponsored research in accordance with the DOE Public Access Plan.

References

1. K. P. Goetz, D. Vermeulen, M. E. Payne, C. Kloc, L. E. McNeil and O. D. Jurchescu, J. Mater. Chem. C, 2014, 2, 3065–3076.
2. S. Horiuchi, F. Ishii, R. Kumai, Y. Okimoto, H. Tachibana, N. Nagaosa and Y. Tokura, Nat. Mater., 2005, 4, 163–166.
3. L. Sun, Y. Wang, F. Yang, X. Zhang and W. Hu, Adv. Mater., 2019, 31, 1902328.
4. S. K. Park, J. H. Kim and S. Y. Park, Adv. Mater., 2018, 30, 1704759.
5. C. Wang, H. Dong, W. Hu, Y. Liu and D. Zhu, Chem. Rev., 2012, 112, 2208–2267.
6. J. Zhang, H. Geng, T. S. Virk, Y. Zhao, J. Tan, C.-A. Di, W. Xu, K. Singh, W. Hu, Z. Shuai, Y. Liu and D. Zhu, Adv. Mater., 2012, 24, 2603–2607.
7. S. Li, Y. Lin and D. Yan, J. Mater. Chem. C, 2016, 4, 2527–2534.
8. P. Majumdar, F. Tharammal, J. Gierschner and S. Varghese, ChemPhysChem, 2020, 21, 616–624.

9. W. Jiang, X. Ma, D. Liu, G. Zhao, W. Tian and Y. Sun, Dyes Pigm., 2021, 193, 109519.
10. Z. Wang and Q. Zhang, Asian J. Org. Chem., 2020, 9, 1252–1261.
11. L. Sun, W. Zhu, F. Yang, B. Li, X. Ren, X. Zhang and W. Hu, Phys. Chem. Chem. Phys. 2018, 20, 6009–6023.
12. D. Yan and D. G. Evans, Mater. Horiz., 2014, 1, 46–57.
13. H.-D. Wu, F.-X. Wang, Y. Xiao and G.-B. Pan, J. Mater. Chem. C, 2014, 2, 2328–2332.
14. Y. Huang, Z. Wang, Z. Chen and Q. Zhang, Angew. Chem., 2019, 58, 9696–9711.
15. A. Mahmood and J.-L. Wang, Energy Environ. Sci., 2021, 14, 90–105.
16. Y. Wu, J. Guo, R. Sun and J. Min, Npj Comput. Mater., 2020, 6, 1–8.
17. S. A. Lopez, B. Sanchez-Lengeling, J. de Goes Soares and A. Aspuru-Guzik, Joule, 2017, 1, 857–870.
18. X. Liu, Y. Shao, T. Lu, D. Chang, M. Li and W. Lu, Mater. Des., 2022, 216, 110561.
19. P. Malhotra, J. C. Verduzco, S. Biswas and G. D. Sharma, ACS Appl. Mater. Interfaces, 2022.
20. W. Shi, T. Deng, Z. M. Wong, G. Wu and S.-W. Yang, Npj Comput. Mater., 2021, 7, 1–8.
21. A. Abou Taka, J. M. Herbert and L. M. McCaslin, ChemRxiv, 2023, DOI: 10.26434/chemrxiv-2023-1xz7b.
22. W. Zhu, L. Zhu, Y. Zou, Y. Wu, Y. Zhen, H. Dong, H. Fu, Z. Wei, Q. Shi and W. Hu. Adv. Mater., 2016, 28, 5954–5962
23. J.-D. Chai and M. Head-Gordon, Phys. Chem. Chem. Phys., 2008, 10, 6615–6620.
24. A. Becke, The quantum theory of atoms in molecules: from solid state to DNA and drug design, John Wiley & Sons, 2007.
25. T. Yanai, D. P. Tew and N. C. Handy, Chem. Phys. Lett., 2004, 393, 51–57.
26. Y. Zhao and D. G. Truhlar, Theor. Chem. Acc., 2008, 120, 215–241.
27. P. C. Hariharan and J. A. Pople, Theor. Chim. Acta, 1973, 28, 213–222.
28. M. J. Frisch, J. A. Pople and J. S. Binkley, J. Chem. Phys., 1984, 80, 3265–3269.
29. K. Raghavachari, J. S. Binkley, R. Seeger and J. A. Pople, J. Chem. Phys., 72 (1980) 650-54.
30. S. Grimme, S. Ehrlich and L. Goerigk, J. Comput. Chem., 2011, 32, 1456–1465.
31. J. Heyd and G. E. Scuseria, J. Chem. Phys., 2004, 121, 1187–1192.
32. E. N. Brothers, A. F. Izmaylov, J. O. Normand, V. Barone and G. Scuseria, J. Chem. Phys., 2008, 129, 011102.
33. R. Bauernschmitt and R. Ahlrichs, Chem. Phys. Lett., 1996, 256, 454–464.
34. M. E. Casida, C. Jamorski, K. C. Casida and D. R. Salahub, J. Chem. Phys., 1998, 108, 4439–4449.
35. R. E. Stratmann, G. E. Scuseria and M. J. Frisch, J. Chem. Phys., 1998, 109, 8218–8224.
36. E. D. Glendening, A. E. Reed, J. E. Carpenter and F. Weinhold, The NBO3.0 Program, 2001, University of Wisconsin, Copyright.
37. F. Plasser. "TheoDORE: A toolbox for a detailed and automated analysis of electronic excited state computations." J. Chem. Phys. 2020, 152, 084108.
38. R. L. Martin, J. Chem. Phys., 2003, 118, 4775–4777.

39. M. J. Frisch, G. W. Trucks, H. B. Schlegel, G. E. Scuseria, M. A. Robb, J. R. Cheeseman, G. Scalmani, V. Barone, G. A. Petersson, H. Nakatsuji, X. Li, M. Caricato, A. V. Marenich, J. Bloino, B. G. Janesko, R. Gomperts, B. Mennucci, H. P. Hratchian, J. V. Ortiz, A. F. Izmaylov, J. L. Sonnenberg, D. Williams-Young, F. Ding, F. Lipparini, F. Egidi, J. Goings, B. Peng, A. Petrone, T. Henderson, D. Ranasinghe, V. G. Zakrzewski, J. Gao, N. Rega, G. Zheng, W. Liang, M. Hada, M. Ehara, K. Toyota, R. Fukuda, J. Hasegawa, M. Ishida, T. Nakajima, Y. Honda, O. Kitao, H. Nakai, T. Vreven, K. Throssell, J. A. Montgomery, Jr., J. E. Peralta, F. Ogliaro, M. J. Bearpark, J. J. Heyd, E. N. Brothers, K. N. Kudin, V. N. Staroverov, T. A. Keith, R. Kobayashi, J. Normand, K. Raghavachari, A. P. Rendell, J. C. Burant, S. S. Iyengar, J. Tomasi, M. Cossi, J. M. Millam, M. Klene, C. Adamo, R. Cammi, J. W. Ochterski, R. L. Martin, K. Morokuma, O. Farkas, J. B. Foresman and D. J. Fox, Gaussian 16 Revision B.01, 2016, Gaussian Inc. Wallingford CT.
40. R. Seeger and J. A. Pople, J. Chem. Phys., 1977, 66, 3045–3050.
41. H. F. Schaefer III and Y. Yamaguchi, J. Mol. Struct.: THEOCHEM , 1986, 135, 369–390.
42. P. Kubelka and F. Munk, “An Article on Optics of Paint Layers”, Z. Tech. Phys. 12, 1931, 593–603.
43. J. I. Pankove, Courier Dover Publications, New York, NY, 1971, Ch. Absorption, pp. 34–52.
44. L. Y. Long, L. S. Liao and S. T. Lee, J. Am. Chem. Soc., 2013, 135, 3744-3747.
45. Z. Weigang, R. Zheng, X. Fu, H. Fu, Q. Shi, Y. Zhen, H. Dong and W. Hu, Angew. Chem. Int. Ed., 2015, 54, 6785-6789.
46. I. Shokaryev, A. Buurma, O. Jurchescu, M. Uijttewaal, G. De Wijs, T. Palstra and R. A. de Groot, J. Phys. Chem. A, 2008, 112, 2497–2502.
47. W. Zhu, Y. Yi, Y. Zhen, and W. Hu, Small, 2015, 11, 2150–2156.
48. A. Bandrauk, K. Truong and C. Carlone, Can. J. Chem., 1982, 60, 588–595.
49. D. Vermeulen, L. Zhu, K. Goetz, P. Hu, H. Jiang, C. Day, O. Jurchescu, V. Coropceanu, C. Kloc and L. McNeil, J. Phys. Chem. C, 2014, 118, 24688–24696.
50. S. Li and D. Yan, Adv. Opt. Mater., 2018, 6, 1800445.
51. Mechanisms and Dynamics of Fluorescence Quenching, ed. J. R. Lakowicz, Springer US, Boston, MA, 2006, pp. 331–351.
52. H. T. Jonkman and J. Kommandeur, Chem. Phys. Lett., 1972, 15, 496–499.
53. I. Haller and F. Kaufman, J. Am. Chem. Soc., 1976, 98, 1464–1468.
54. L. Ma, P. Hu, C. Kloc, H. Sun, M. E. Michel-Beyerle, and G. G. Gurzadyan, Chem. Phys. Lett., 2014, 609, 11–14.
55. N. M. Monezi and R. A. Ando, Vib. Spectrosc., 2018, 99, 67–72.
56. R. S. Mulliken, J. Am. Chem. Soc., 1952, 74, 811–824.

Supporting Information:

Comparing the Structures and Photophysical Properties of Two Charge Transfer Co-crystals

Ali Abou Taka,[†] Joseph E. Reynolds III,[†] Neil C. Cole-Filipiak,[†] Mohana Shivanna,[†] Christine J. Yu,[‡] Patrick Feng,[†] Mark D. Allendorf,[†] Krupa Ramasesha,[†] Vitalie Stavila,[†] and Laura M. McCaslin*,[†]

†*Combustion Research Facility, Sandia National Laboratories, Livermore, California 94550, USA*

‡*Department of Chemistry, Northwestern University, Evanston, Illinois 60208, USA*

E-mail: lmmccas@sandia.gov

Contents

1 Experimental Results

1.1 Figures

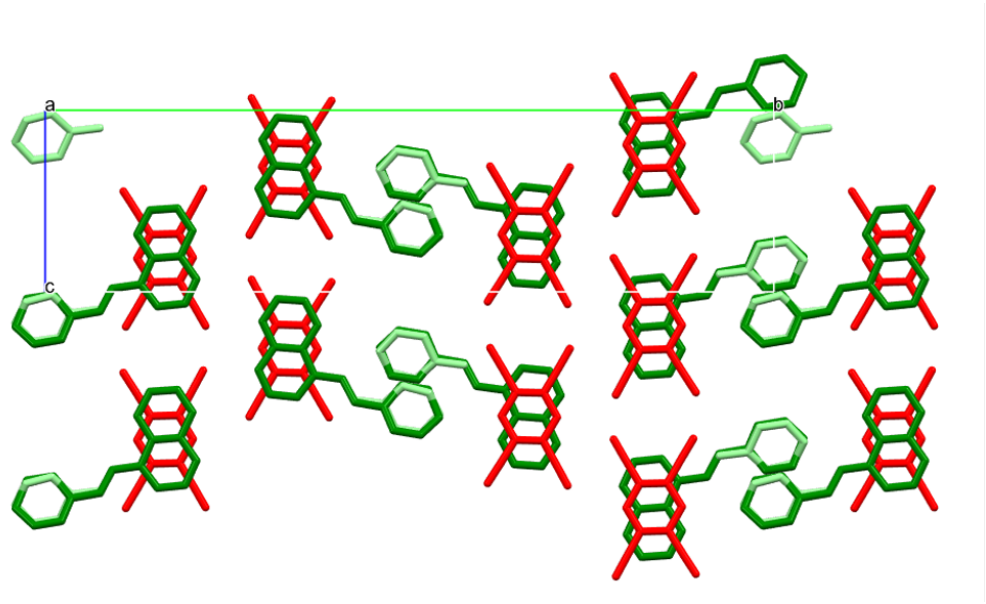

Figure S1: Expanded unit cell of Npe:TCNB (view along the crystallographic a-axis).

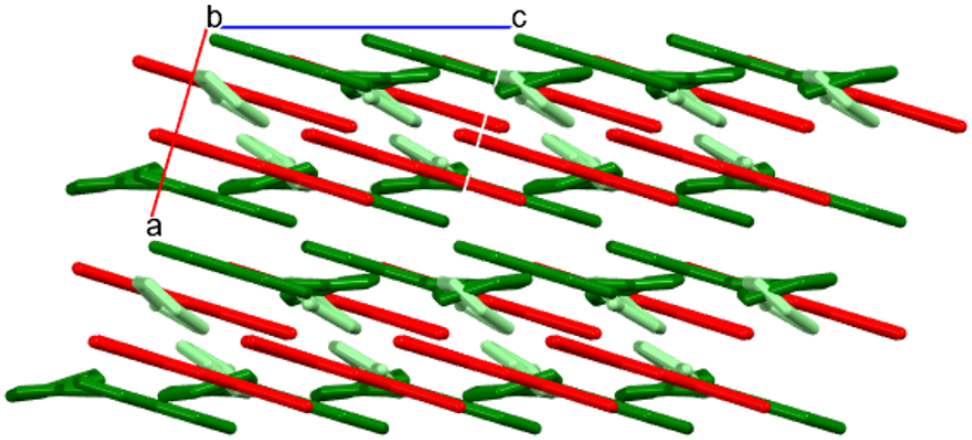

Figure S2: Expanded unit cell of Npe:TCNB (view along the crystallographic b-axis).

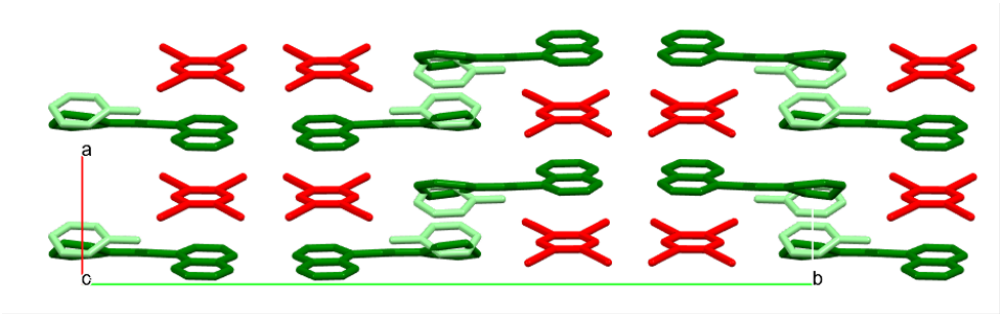

Figure S3: Expanded unit cell of Npe:TCNB (view along the crystallographic c-axis).

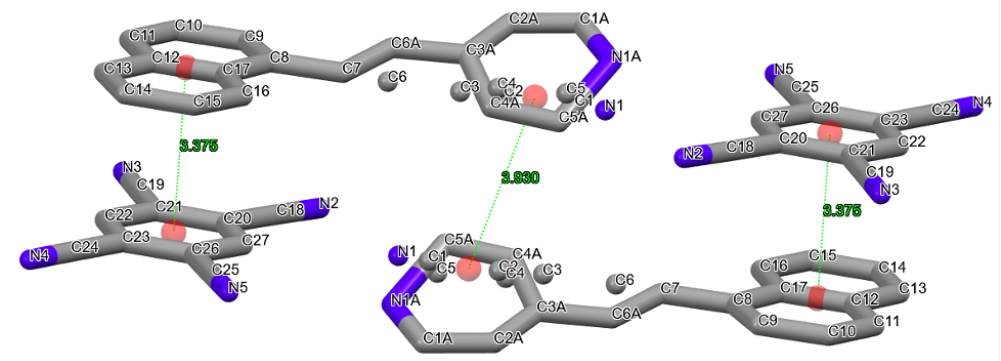

Figure S4: Expanded asymmetric unit of Npe:TCNB (interatomic distances in Å).

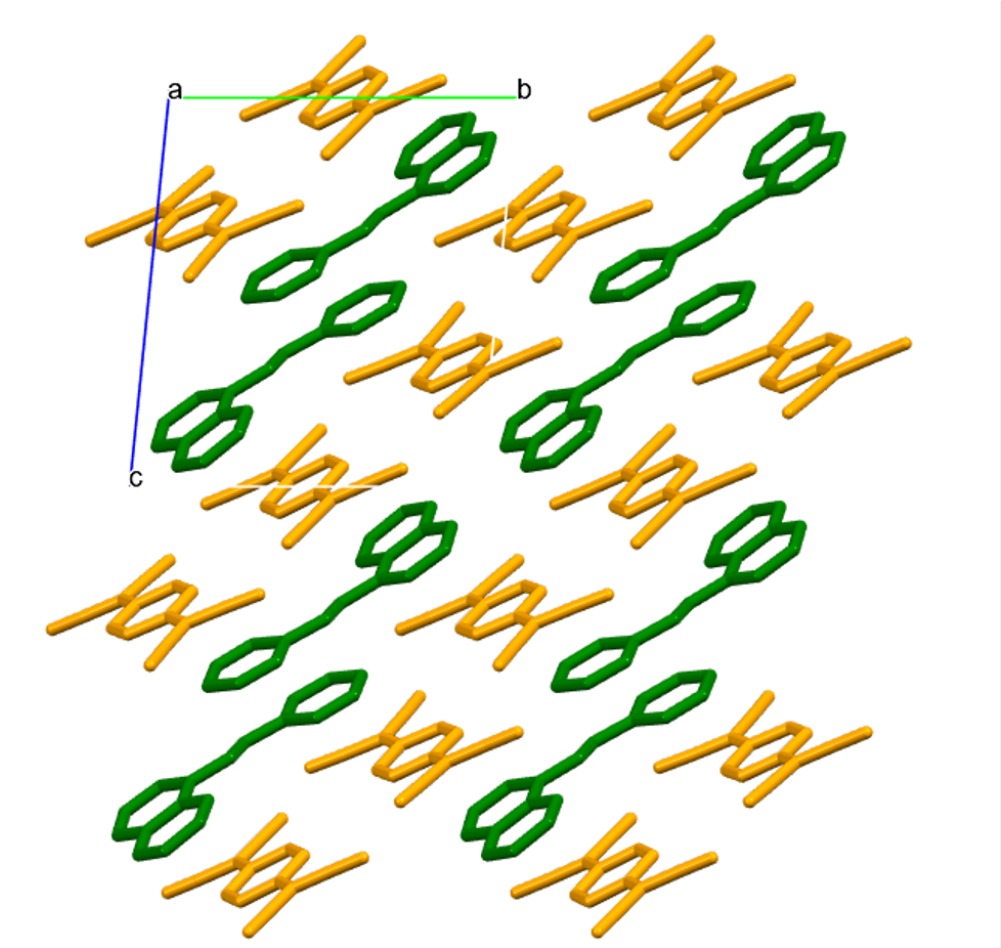

Figure S5: Expanded unit cell of Npe:TCNQ (view along the crystallographic a-axis).

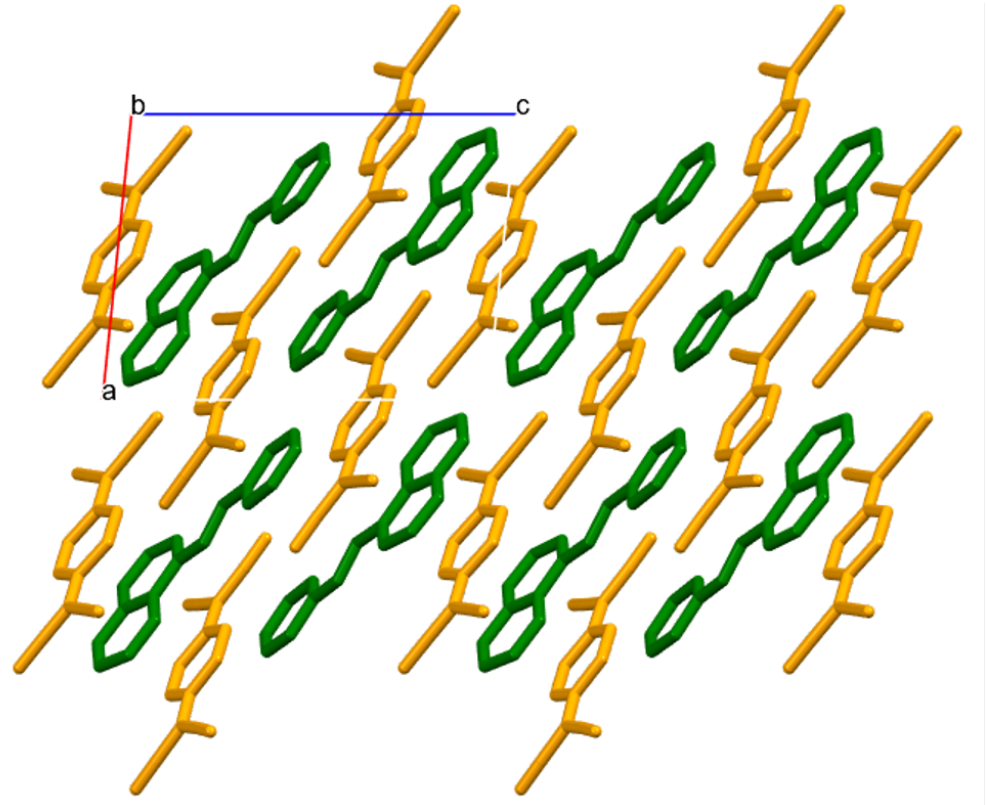

Figure S6: Expanded unit cell of Npe:TCNQ (view along the crystallographic b-axis).

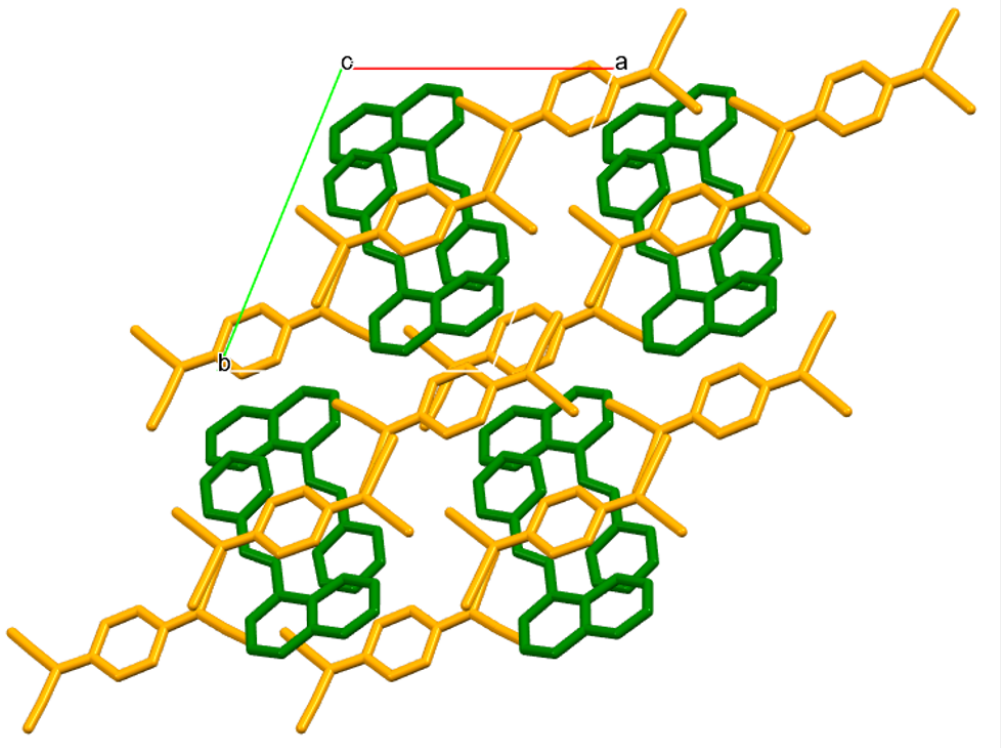

Figure S7: Expanded unit cell of Npe:TCNQ (view along the crystallographic c-axis).

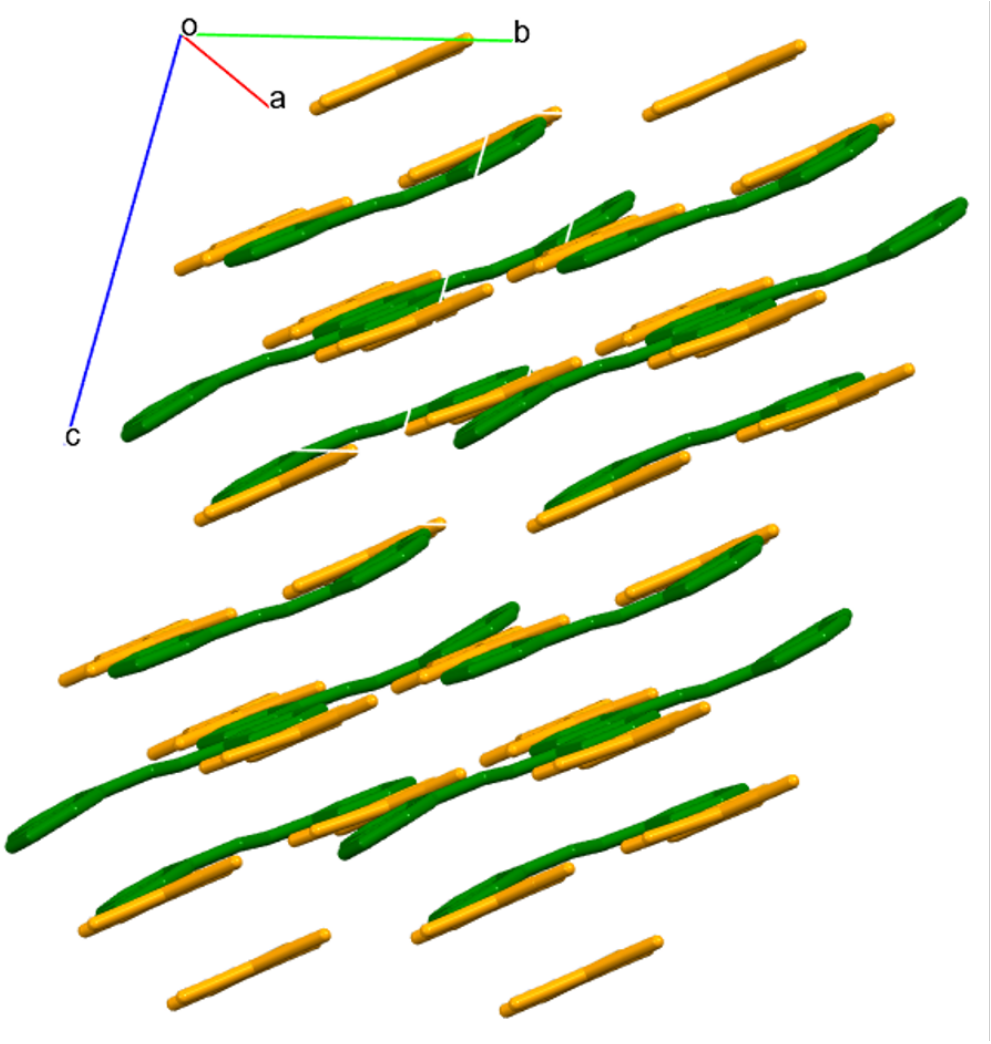

Figure S8: Expanded unit cell of Npe:TCNQ (view along off angle to show layered structure).

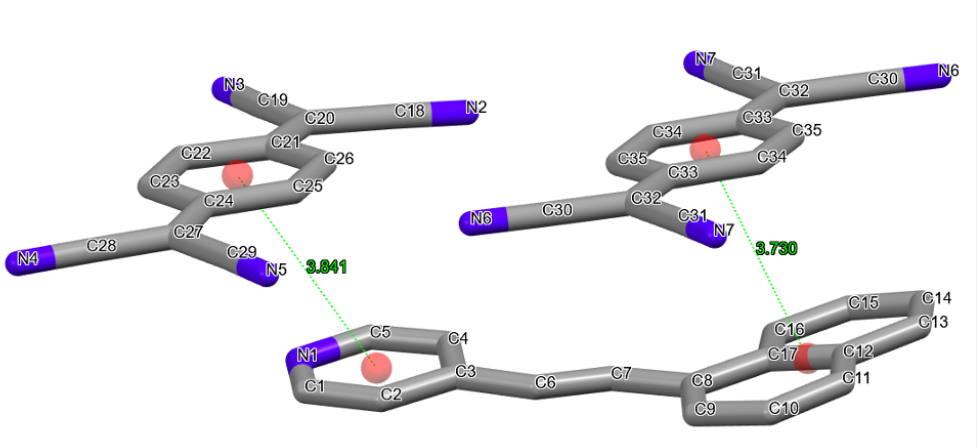

Figure S9: Expanded asymmetric unit of Npe:TCNQ (interatomic distances in Å).

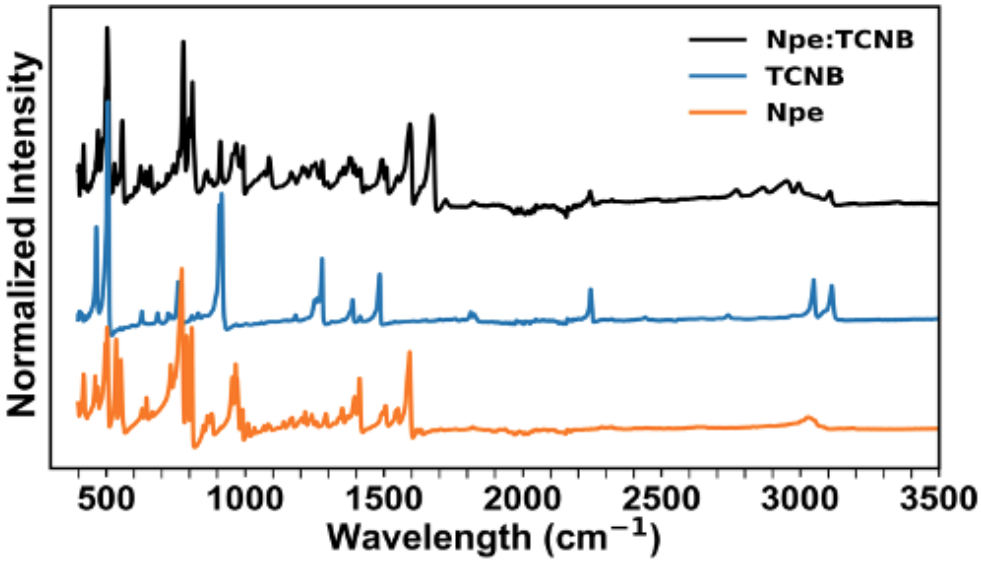

Figure S10: Infrared spectra of Npe, TCNB, and Npe:TCNB co-crystals.

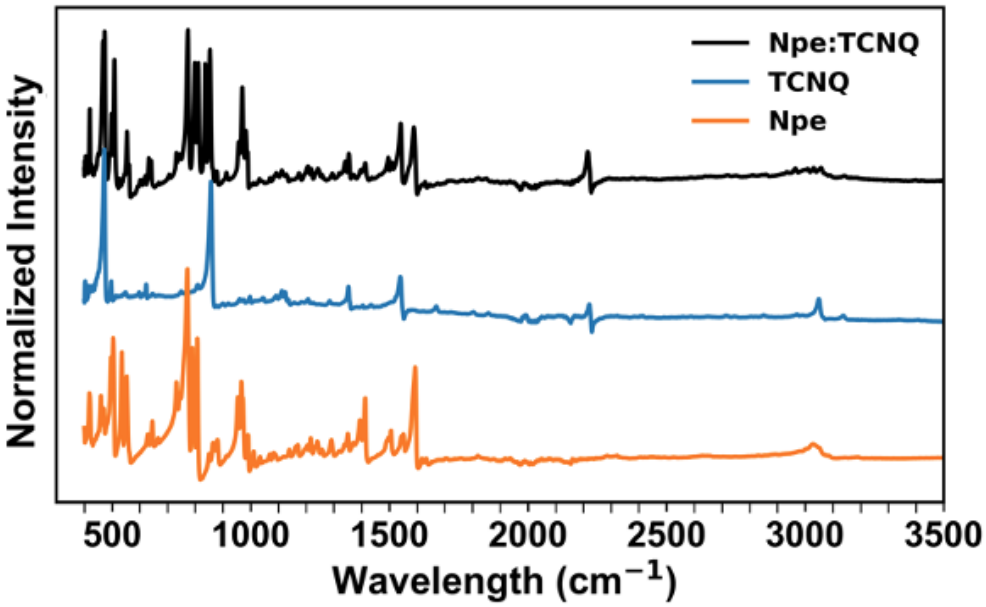

Figure S11: Infrared spectra of Npe, TCNQ, and Npe:TCNQ co-crystals.

1.2 Band Gap Analysis

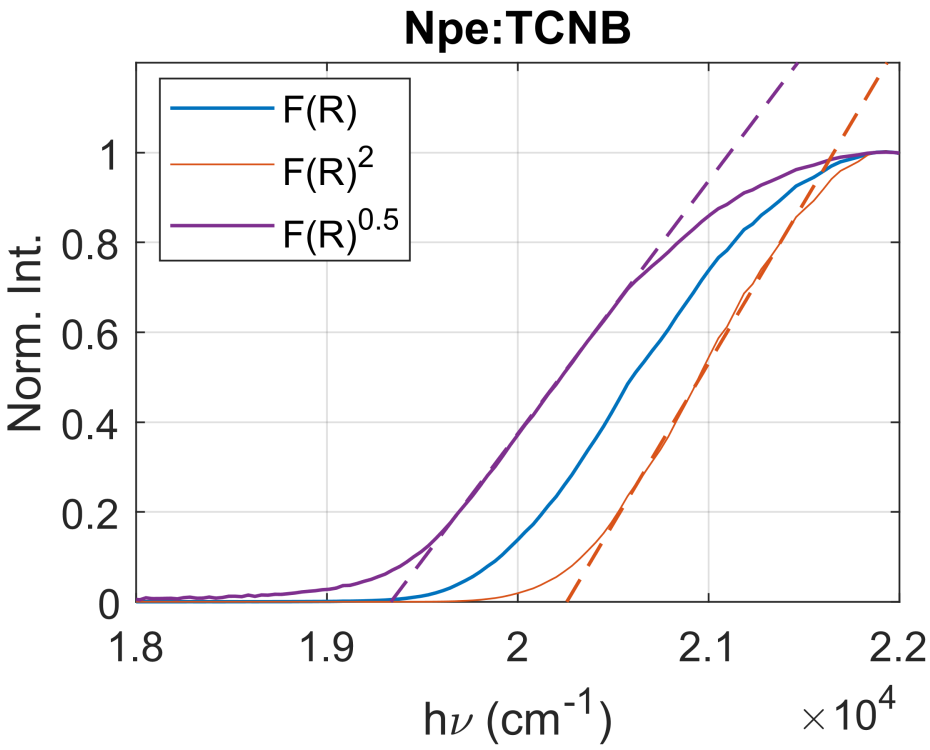

Figure S12: Plots of $F(R)1/\gamma$ vs. photon energy for Npe:TCNB.

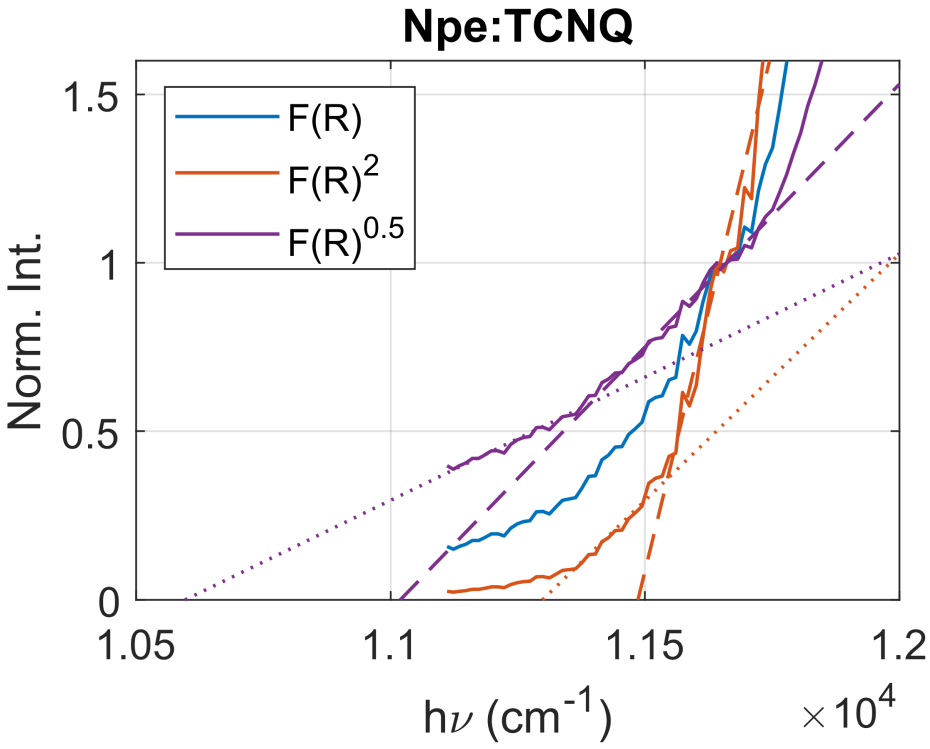

Figure S13: Plots of $F(R)1/\gamma$ vs. photon energy for Npe:TCNQ. Due to the vibronic structure observed in Npe:TCNQ, multiple linear fits were performed up to the lowest energy shoulder at 11600 cm^{-1}.

2 Computational Results

2.1 Figures

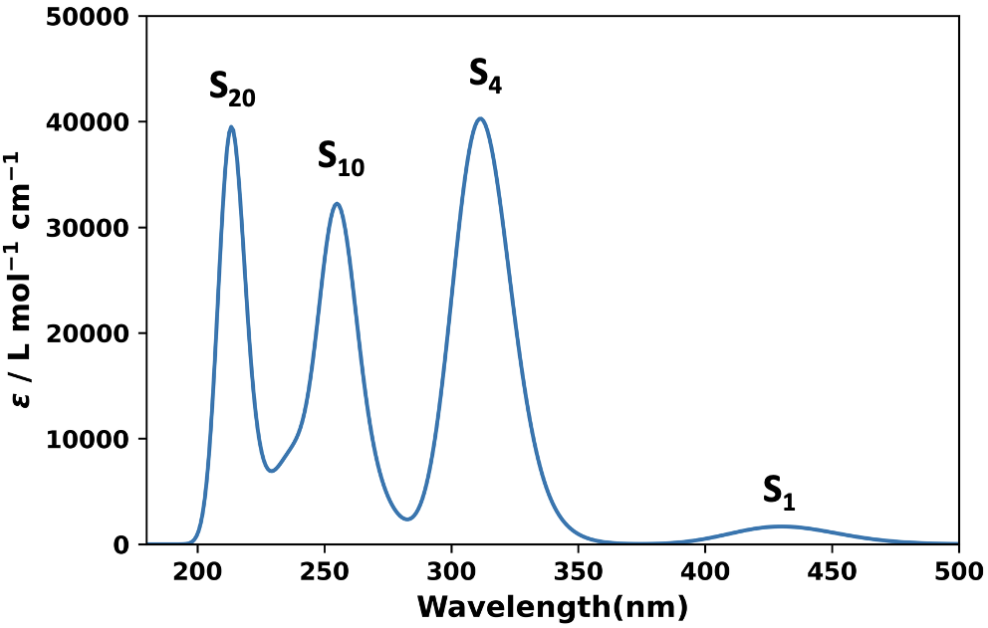

Figure S14: Simulated UV-Vis absorption spectra of Npe:TCNB conformer a, computed with CAM-B3LYP-D3/6-31+G(d,p).

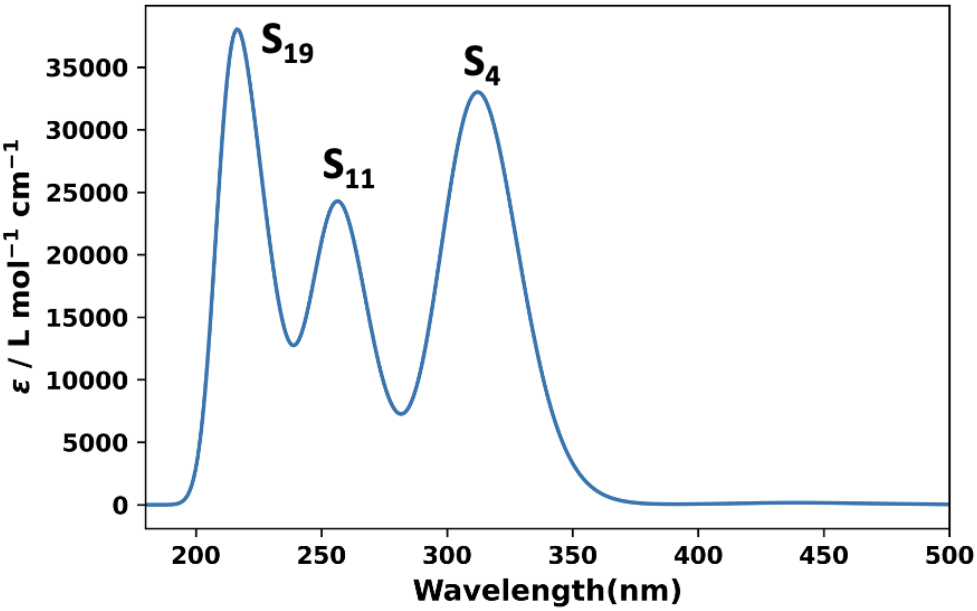

Figure S15: Simulated UV-Vis absorption spectra of Npe:TCNB conformer b, computed with CAM-B3LYP-D3/6-31+G(d,p).

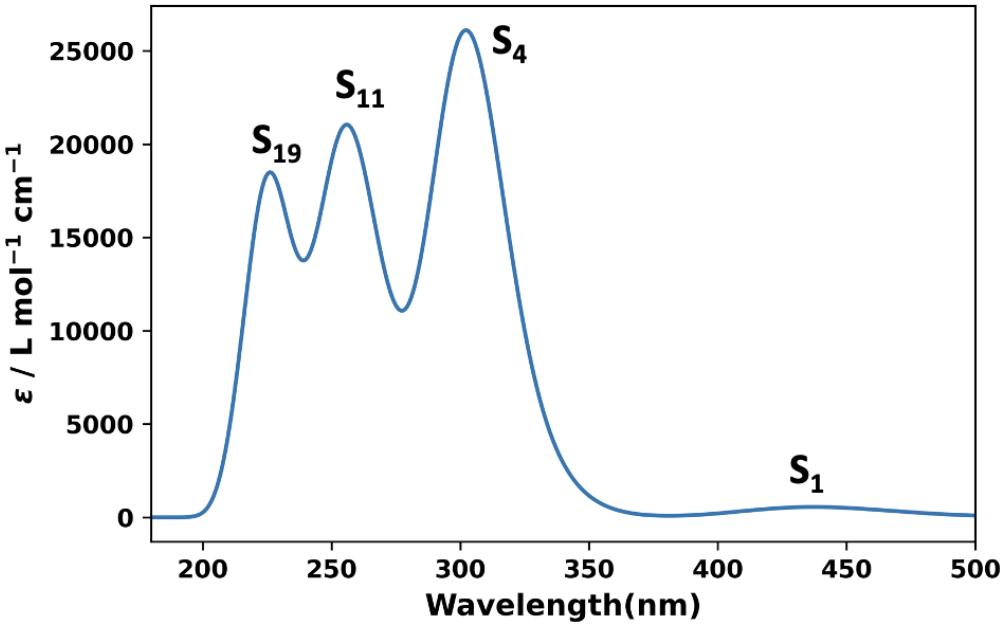

Figure S16: Simulated UV-Vis absorption spectra of Npe:TCNB conformer c, computed with CAM-B3LYP-D3/6-31+G(d,p).

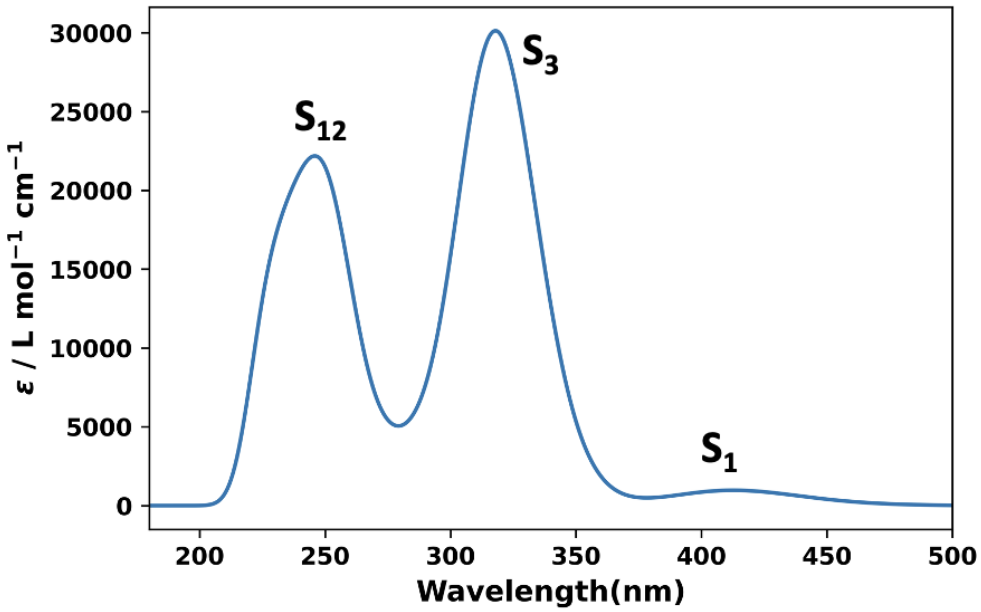

Figure S17: Simulated UV-Vis absorption spectra of Npe:TCNB conformer d, computed with CAM-B3LYP-D3/6-31+G(d,p).

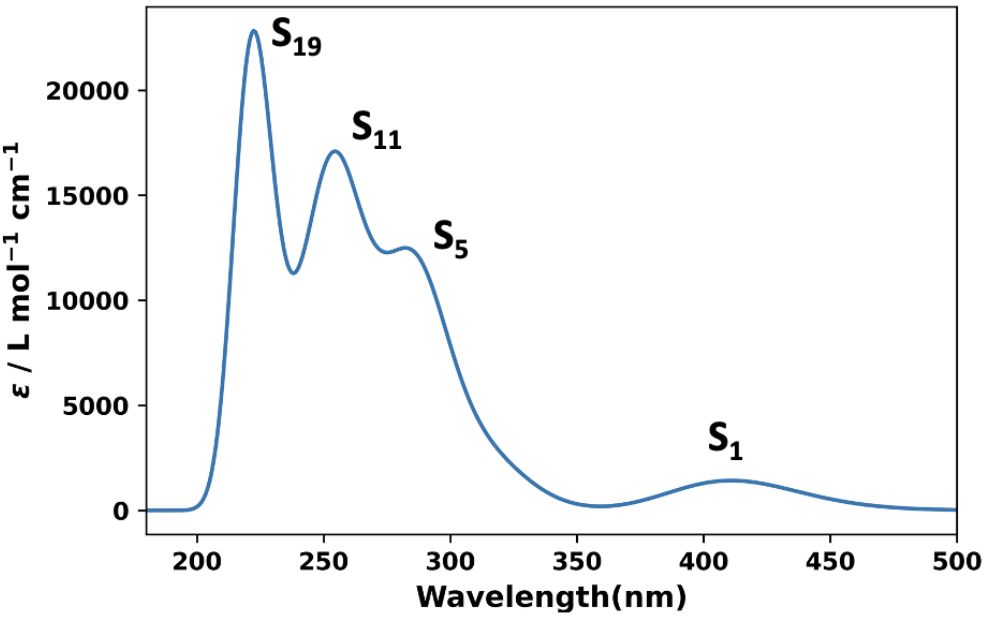

Figure S18: Simulated UV-Vis absorption spectra of Npe:TCNB conformer e, computed with CAM-B3LYP-D3/6-31+G(d,p).

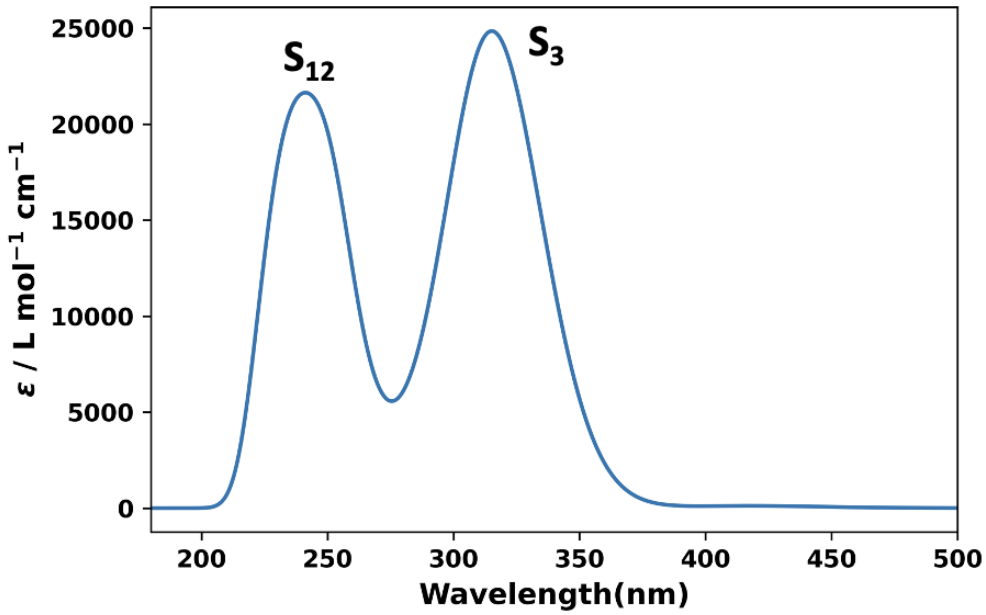

Figure S19: Simulated UV-Vis absorption spectra of Npe:TCNB conformer f, computed with CAM-B3LYP-D3/6-31+G(d,p).

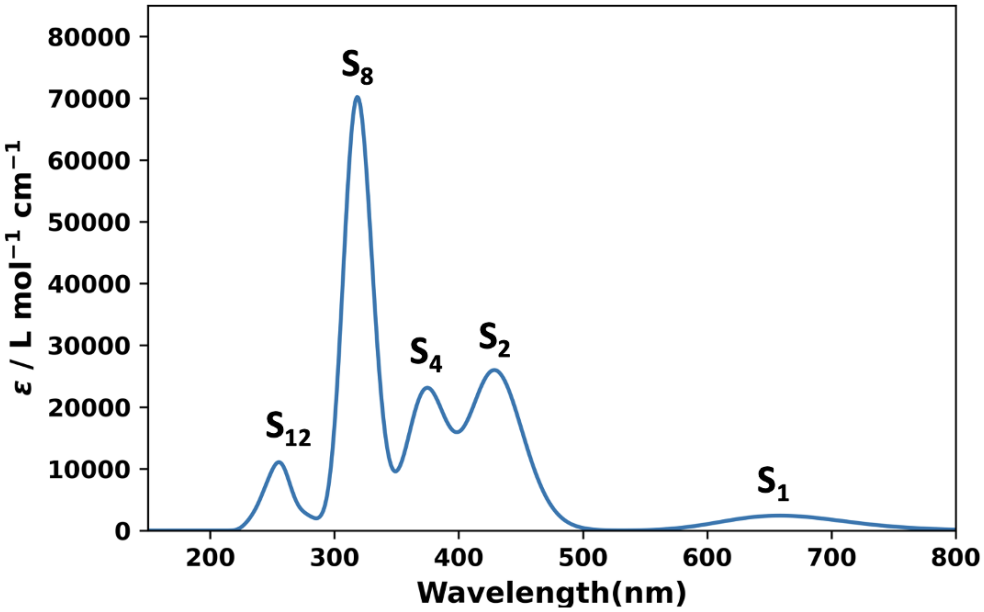

Figure S20: Simulated UV-Vis absorption spectra of Npe:TCNQ conformer a, computed with CAM-B3LYP-D3/6-31+G(d,p).

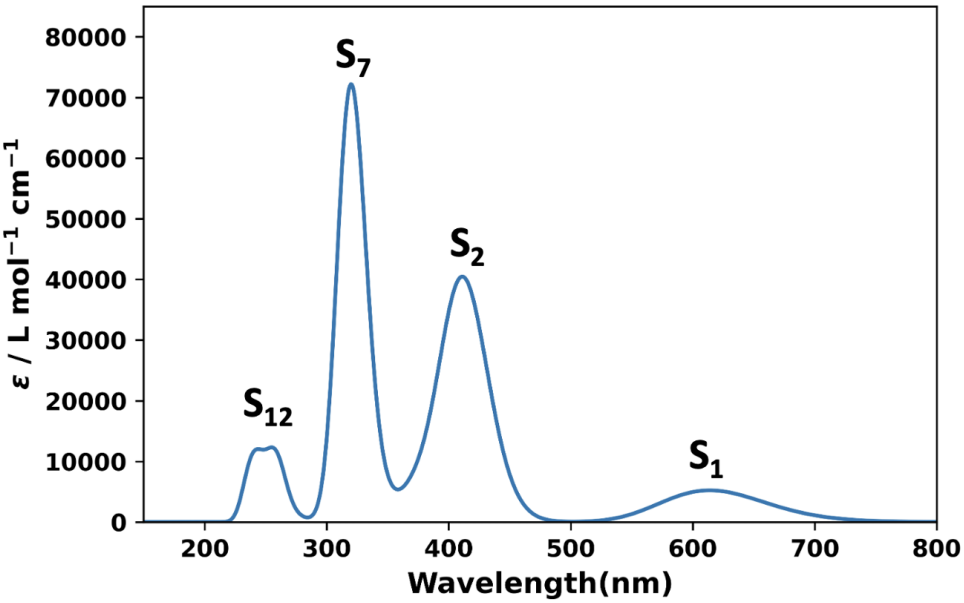

Figure S21: Simulated UV-Vis absorption spectra of Npe:TCNQ conformer b, computed with CAM-B3LYP-D3/6-31+G(d,p).

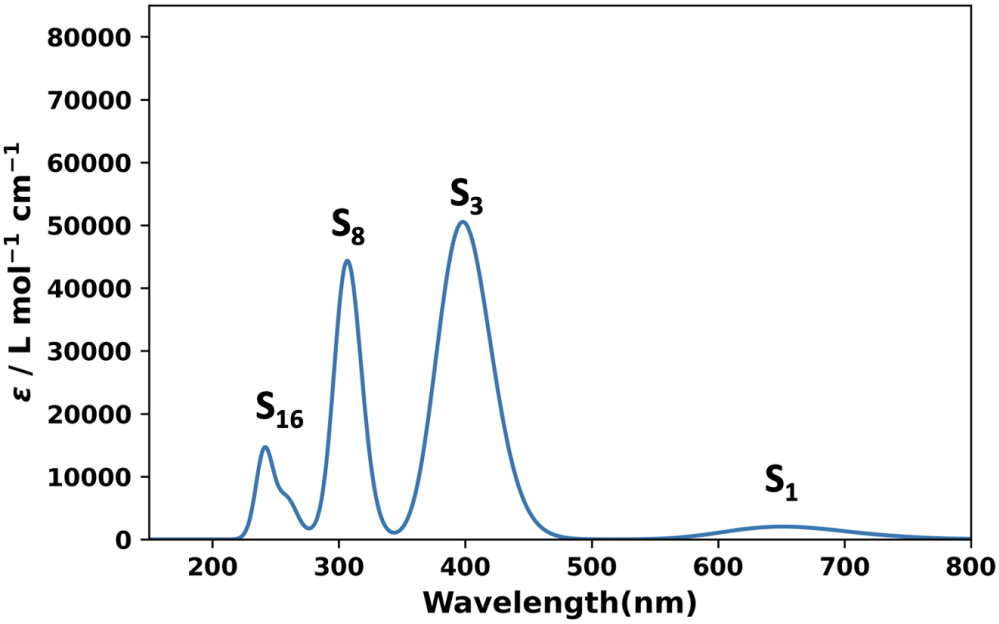

Figure S22: Simulated UV-Vis absorption spectra of Npe:TCNQ conformer c, computed with CAM-B3LYP-D3/6-31+G(d,p).

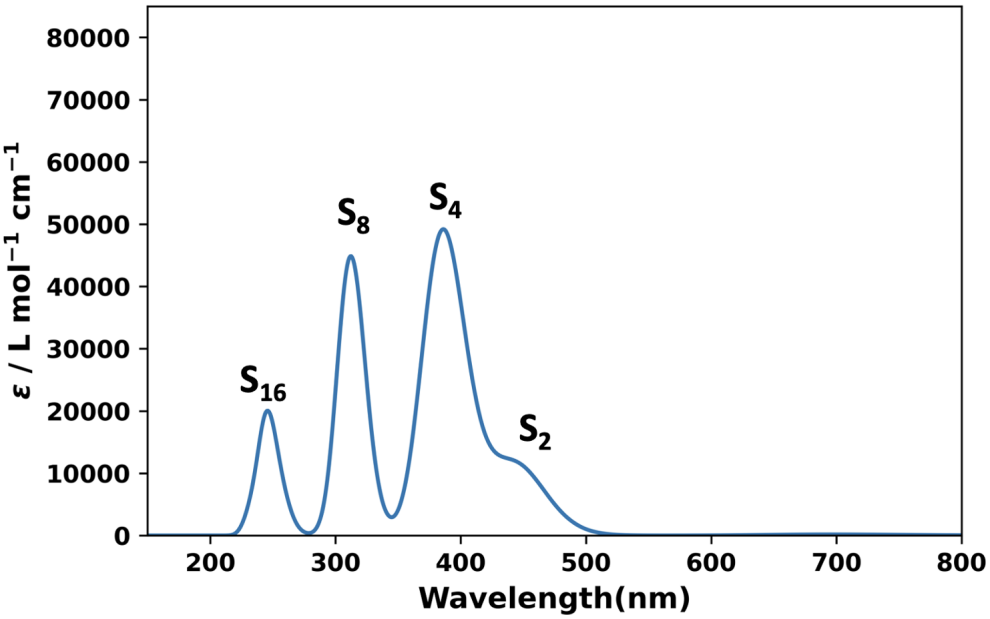

Figure S23: Simulated UV-Vis absorption spectra of Npe:TCNQ conformer d, computed with CAM-B3LYP-D3/6-31+G(d,p).

2.2 Energetics

Table S1: Relative energies of Npe:TCNQ conformers optimized with different functionals and basis sets. All relative energies are zero-point energy corrected.

Model Chemistry / Conformer	a	b	c	d
B3LYP/6-31G(d,p)	0.000	0.096	0.014	0.014
B3LYP/6-31+G(d,p)	0.016	0.000	0.029	0.027
B3LYP/6-311+G(d,p)	0.017	0.000	N/A	0.024
B3LYP-D3/6-31G(d,p)	0.016	0.000	0.077	0.106
B3LYP-D3/6-31+G(d,p)	0.008	0.000	0.074	0.102
B3LYP-D3/6-311+G(d,p)	0.007	0.000	0.077	0.104
CAM-B3LYP/6-31G(d,p)	0.000	0.080	0.068	0.019
CAM-B3LYP/6-31+G(d,p)	0.006	0.059	0.000	0.000
CAM-B3LYP/6-311+G(d,p)	0.004	0.056	0.000	0.000
CAM-B3LYP-D3/6-31G(d,p)	0.000	0.003	0.024	0.028
CAM-B3LYP-D3/6-31+G(d,p)	0.000	0.010	0.026	0.029
CAM-B3LYP-D3/6-311+G(d,p)	0.000	0.010	0.031	0.034
ωB97X-D/6-31G(d,p)	0.003	0.000	0.006	0.018
ωB97X-D/6-31+G(d,p)	0.000	0.006	0.017	0.032
ωB97X-D/6-311+G(d,p)	0.000	0.011	0.024	0.035
M062x/6-31G(d,p)	0.012	0.000	0.040	0.055
M062x/6-31+G(d,p)	0.013	0.000	0.042	0.054
M062x/6-311+G(d,p)	0.010	0.000	0.048	0.062

Table S2: Relative energies of Npe:TCNB conformers optimized with different functionals and basis sets. All relative energies are zero-point energy corrected.

Model Chemistry / Conformer	a	b	c	d	e	f
B3LYP/6-31G(d,p)	0.000	0.005	0.073	0.023	0.235	0.083
B3LYP/6-31+G(d,p)	0.000	0.002	0.075	N/A	0.215	0.078
B3LYP/6-311+G(d,p)	0.000	0.002	0.073	N/A	0.208	0.024
B3LYP-D3/6-31G(d,p)	0.000	0.015	0.059	0.113	0.129	0.182
B3LYP-D3/6-31+G(d,p)	0.000	0.009	0.063	0.121	0.110	0.190
B3LYP-D3/6-311+G(d,p)	0.000	0.013	0.066	0.129	0.106	0.203
CAM-B3LYP/6-31G(d,p)	0.000	0.004	0.069	0.040	0.208	0.119
CAM-B3LYP/6-31+G(d,p)	0.000	0.000	0.071	0.011	0.183	0.103
CAM-B3LYP/6-311+G(d,p)	0.000	0.000	0.070	0.037	0.178	0.108
CAM-B3LYP-D3/6-31G(d,p)	0.000	0.016	0.060	0.103	0.133	0.171
CAM-B3LYP-D3/6-31+G(d,p)	0.000	0.009	0.062	0.107	0.111	0.179
CAM-B3LYP-D3/6-311+G(d,p)	0.000	0.014	0.064	0.115	0.106	0.190
ωB97X-D/6-31G(d,p)	0.000	0.017	0.055	0.114	0.113	0.182
ωB97X-D/6-31+G(d,p)	0.000	0.012	0.054	0.120	0.083	0.181
ωB97X-D/6-311+G(d,p)	0.000	0.018	0.061	0.130	0.082	0.200
M062x/6-31G(d,p)	0.000	0.015	0.053	0.129	0.132	0.191
M062x/6-31+G(d,p)	0.000	0.012	0.054	0.136	0.108	0.204
M062x/6-311+G(d,p)	0.000	0.015	0.055	0.153	0.099	0.221

2.3 Excited State Properties

2.3.1 Npe:TCNQ

Table S3: Excitation energies and oscillator strengths of Npe:TCNQ conformer a at the CAM-B3LYP-D3/6-31+G(d,p) level of theory

Excited State	Oscillator Strength	E (eV)	E (nm)
S1	0.030	1.884	658.24
S2	0.310	2.884	429.93
S3	0.015	3.035	408.45
S4	0.280	3.315	374.00
S5	0.001	3.629	341.65
S6	0.008	3.783	327.71
S7	0.000	3.810	325.42
S8	0.860	3.894	318.40
S9	0.011	4.435	279.54
S10	0.014	4.479	276.78
S11	0.003	4.653	266.48
S12	0.076	4.789	258.89
S13	0.036	4.863	254.95
S14	0.015	4.942	250.88
S15	0.010	4.993	248.30
S16	0.017	5.073	244.40
S17	0.028	5.086	243.77
S18	0.000	5.221	237.46
S19	0.017	5.311	233.44
S20	0.000	5.351	231.68

Table S4: Excitation energies and oscillator strengths of Npe:TCNQ conformer b at the CAM-B3LYP-D3/6-31+G(d,p) level of theory

Excited State	Oscillator Strength	E (eV)	E (nm)
S1	0.065	2.020	613.83
S2	0.489	3.010	411.95
S3	0.002	3.121	397.30
S4	0.071	3.299	375.79
S5	0.033	3.648	339.88
S6	0.002	3.748	330.83
S7	0.879	3.876	319.88
S8	0.002	3.945	314.25
S9	0.004	4.441	279.19
S10	0.003	4.493	275.97
S11	0.003	4.671	265.42
S12	0.091	4.772	259.80
S13	0.032	4.848	255.72
S14	0.006	4.901	252.98
S15	0.046	5.011	247.44
S16	0.043	5.122	242.06
S17	0.025	5.156	240.45
S18	0.038	5.244	236.43
S19	0.000	5.250	236.16
S20	0.022	5.308	233.57

Table S5: Excitation energies and oscillator strengths of Npe:TCNQ conformer c at the CAM-B3LYP-D3/6-31+G(d,p) level of theory

Excited State	Oscillator Strength	E (eV)	E (nm)
S1	0.025	1.905	651.01
S2	0.066	2.947	420.74
S3	0.418	3.080	402.50
S4	0.243	3.219	385.20
S5	0.001	3.713	333.89
S6	0.003	3.743	331.28
S7	0.001	3.885	319.13
S8	0.547	4.042	306.76
S9	0.011	4.389	282.48
S10	0.000	4.502	275.38
S11	0.003	4.755	260.73
S12	0.070	4.777	259.57
S13	0.002	4.867	254.74
S14	0.011	5.063	244.90
S15	0.036	5.090	243.59
S16	0.125	5.143	241.09
S17	0.001	5.227	237.19
S18	0.008	5.237	236.74
S19	0.004	5.332	232.54
S20	0.005	5.367	231.01

Table S6: Excitation energies and oscillator strengths of Npe:TCNQ conformer d at the CAM-B3LYP-D3/6-31+G(d,p) level of theory

Excited State	Oscillator Strength	E (eV)	E (nm)
S1	0.002	1.782	695.55
S2	0.135	2.788	444.76
S3	0.051	3.084	402.07
S4	0.573	3.220	385.09
S5	0.003	3.624	342.13
S6	0.000	3.715	333.78
S7	0.003	3.873	320.12
S8	0.552	3.971	312.25
S9	0.000	4.450	278.64
S10	0.001	4.476	277.02
S11	0.003	4.706	263.44
S12	0.027	4.800	258.32
S13	0.043	4.863	254.94
S14	0.029	5.006	247.66
S15	0.034	5.052	245.43
S16	0.145	5.061	244.99
S17	0.002	5.193	238.75
S18	0.022	5.207	238.10
S19	0.013	5.307	233.62
S20	0.026	5.346	231.94

2.3.2 Npe:TCNB

Table S7: Excitation energies and oscillator strengths of Npe:TCNB conformer a at the CAM-B3LYP-D3/6-31+G(d,p) level of theory

Excited State	Oscillator Strength	E (eV)	E (nm)
S1	0.021	2.883	430.05
S2	0.020	3.738	331.66
S3	0.017	3.884	319.25
S4	0.478	3.985	311.14
S5	0.006	4.202	295.09
S6	0.001	4.503	275.34
S7	0.040	4.577	270.91
S8	0.003	4.701	263.76
S9	0.013	4.795	258.58
S10	0.356	4.859	255.16
S11	0.004	4.882	253.95
S12	0.005	4.931	251.44
S13	0.024	5.042	245.90
S14	0.010	5.056	245.21
S15	0.000	5.108	242.71
S16	0.082	5.246	236.35
S17	0.002	5.366	231.06
S18	0.000	5.474	226.51
S19	0.049	5.542	223.71
S20	0.480	5.814	213.23

Table S8: Excitation energies and oscillator strengths of Npe:TCNB conformer b at the CAM-B3LYP-D3/6-31+G(d,p) level of theory

Excited State	Oscillator Strength	E (eV)	E (nm)
S1	0.003	2.823	439.18
S2	0.026	3.778	328.21
S3	0.066	3.881	319.46
S4	0.463	3.986	311.07
S5	0.012	4.154	298.50
S6	0.003	4.498	275.61
S7	0.063	4.575	271.01
S8	0.003	4.684	264.68
S9	0.019	4.770	259.92
S10	0.033	4.795	258.55
S11	0.209	4.821	257.20
S12	0.090	4.899	253.09
S13	0.004	4.988	248.56
S14	0.021	5.018	247.09
S15	0.020	5.069	244.61
S16	0.030	5.220	237.53
S17	0.019	5.385	230.23
S18	0.001	5.486	226.00
S19	0.257	5.495	225.65
S20	0.526	5.786	214.28

Table S9: Excitation energies and oscillator strengths of Npe:TCNB conformer c at the CAM-B3LYP-D3/6-31+G(d,p) level of theory

Excited State	Oscillator Strength	E (eV)	E (nm)
S1	0.009	2.835	437.33
S2	0.022	3.771	328.82
S3	0.025	3.908	317.25
S4	0.358	4.106	301.99
S5	0.050	4.131	300.10
S6	0.001	4.507	275.11
S7	0.084	4.581	270.65
S8	0.018	4.730	262.14
S9	0.010	4.754	260.80
S10	0.013	4.783	259.24
S11	0.131	4.829	256.75
S12	0.109	4.893	253.39
S13	0.018	4.932	251.40
S14	0.018	5.062	244.94
S15	0.030	5.104	242.92
S16	0.054	5.275	235.06
S17	0.017	5.349	231.77
S18	0.011	5.495	225.63
S19	0.216	5.498	225.52
S20	0.074	5.744	215.86

Table S10: Excitation energies and oscillator strengths of Npe:TCNB conformer d at the CAM-B3LYP-D3/6-31+G(d,p) level of theory

Excited State	Oscillator Strength	E (eV)	E (nm)
S1	0.016	3.005	412.63
S2	0.187	3.865	320.75
S3	0.305	3.912	316.91
S4	0.006	4.148	298.87
S5	0.014	4.299	288.42
S6	0.033	4.305	288.01
S7	0.001	4.499	275.56
S8	0.002	4.514	274.68
S9	0.035	4.616	268.59
S10	0.003	4.763	260.30
S11	0.004	4.795	258.57
S12	0.230	4.910	252.54
S13	0.017	4.989	248.54
S14	0.012	5.064	244.84
S15	0.019	5.179	239.41
S16	0.084	5.187	239.04
S17	0.085	5.196	238.59
S18	0.004	5.308	233.60
S19	0.169	5.471	226.64
S20	0.001	5.504	225.27

Table S11: Excitation energies and oscillator strengths of Npe:TCNB conformer e at the CAM-B3LYP-D3/6-31+G(d,p) level of theory

Excited State	Oscillator Strength	E (eV)	E (nm)
S1	0.023	3.018	410.88
S2	0.007	3.898	318.04
S3	0.027	3.927	315.71
S4	0.004	4.133	299.95
S5	0.165	4.315	287.33
S6	0.003	4.556	272.12
S7	0.058	4.583	270.52
S8	0.006	4.776	259.60
S9	0.100	4.799	258.36
S10	0.012	4.803	258.16
S11	0.113	4.928	251.62
S12	0.014	4.955	250.22
S13	0.023	5.069	244.60
S14	0.007	5.094	243.38
S15	0.011	5.126	241.89
S16	0.035	5.198	238.52
S17	0.026	5.434	228.15
S18	0.004	5.471	226.63
S19	0.270	5.566	222.74
S20	0.088	5.675	218.49

Table S12: Excitation energies and oscillator strengths of Npe:TCNB conformer f at the CAM-B3LYP-D3/6-31+G(d,p) level of theory

Excited State	Oscillator Strength	E (eV)	E (nm)
S1	0.002	2.967	417.84
S2	0.191	3.793	326.89
S3	0.260	3.994	310.46
S4	0.003	4.117	301.16
S5	0.068	4.260	291.08
S6	0.000	4.281	289.61
S7	0.002	4.463	277.77
S8	0.002	4.480	276.77
S9	0.035	4.604	269.30
S10	0.004	4.754	260.80
S11	0.005	4.814	257.56
S12	0.180	4.919	252.03
S13	0.051	4.997	248.12
S14	0.003	5.042	245.91
S15	0.004	5.176	239.55
S16	0.047	5.203	238.29
S17	0.157	5.234	236.89
S18	0.009	5.326	232.80
S19	0.000	5.438	227.98
S20	0.142	5.478	226.35

2.4 Geometries

2.4.1 Monomer Optimized Geometries

Npe

E=-709.793714 E_h

0 1

H	-0.77115	-0.799086	0.879519
H	-0.87117	1.741053	-0.814270
H	-5.38473	-1.529269	1.558058
H	-5.34332	1.108336	-1.594221
N	-5.48399	-0.210198	-0.019065
H	-2.91635	-1.467138	1.760004
C	-4.79778	-0.908312	0.886069
H	-2.88553	1.277052	-1.555187
C	-4.77316	0.552246	-0.854454
C	-3.41319	-0.874530	0.998251
C	-3.38982	0.654042	-0.825180
C	-2.66965	-0.067860	0.132785
C	-1.20767	-0.021327	0.258901
C	-0.41240	0.915132	-0.274255
H	4.46426	-3.093441	-0.164285
H	2.07143	-3.461807	-0.755678
H	0.49422	-1.600252	-0.754509
C	3.77175	-2.258173	-0.161917
C	2.41284	-2.467786	-0.485571
H	0.89869	3.135538	0.072813
C	1.52429	-1.423750	-0.475151
C	4.21212	-0.995547	0.129999
H	4.85043	1.564254	0.592439
H	3.30679	3.495529	0.509980
H	5.25925	-0.815125	0.354509
C	1.57026	2.282074	0.081861
C	1.04788	1.019981	-0.115663
C	1.93826	-0.106187	-0.141090
C	3.32075	0.108878	0.132821
C	3.79480	1.421207	0.382219
C	2.93989	2.489203	0.337756

TCNB

E=-600.830452 E_h

0 1

N	3.41977	2.049057	-0.000007
C	2.43855	1.438636	0.000008
N	3.41977	-2.049060	0.000033
C	2.43855	-1.438636	-0.000029
N	-3.41979	2.049011	0.000000
C	-2.43855	1.438627	0.000010
N	-3.41978	-2.049018	0.000024
C	-2.43855	-1.438624	-0.000028
H	0.00001	2.479386	0.000011
H	0.00000	-2.479384	-0.000015
C	1.20749	-0.703056	-0.000010
C	1.20749	0.703057	0.000001
C	0.00000	1.396228	0.000005
C	-1.20747	0.703065	0.000002
C	-1.20747	-0.703061	-0.000011
C	0.00000	-1.396225	-0.000006

TCNQ

E=-678.139475 E_h

0 1

C	3.55427	-0.101710	-1.200959
C	3.12639	-2.070474	0.155950
C	2.63650	-0.857155	-0.412279
C	1.33424	-0.433766	-0.208625
H	1.53135	1.388635	-1.393966
C	0.85381	0.795466	-0.790202
H	-0.76546	2.135349	-1.034813
C	-0.41817	1.208998	-0.591304
N	4.28461	0.525477	-1.844522
N	3.50560	-3.058588	0.625799
C	-3.55427	0.101710	1.200959
C	-3.12639	2.070474	-0.155950
C	-2.63650	0.857155	0.412279
C	-1.33424	0.433766	0.208625
H	-1.53135	-1.388635	1.393966
C	-0.85381	-0.795466	0.790202
H	0.76546	-2.135349	1.034813
C	0.41817	-1.208998	0.591304
N	-4.28461	-0.525477	1.844522
N	-3.50560	3.058588	-0.625799

2.4.2 Npe:TCNQ Optimized Geometries

Npe:TCNQ conformer a

SCF=-1388.27454303 E_h

0 1

H	-4.55633	-1.783357	-2.256453
N	6.29838	-0.505046	-1.267842
H	6.85494	0.169781	0.595166
C	6.03539	-0.240235	0.010943
H	5.52737	-1.217057	-3.039312
C	5.29845	-1.006754	-1.997921
C	-4.33553	1.507465	-1.564542
C	-4.66333	0.920872	0.773552
C	-3.76942	1.326246	-0.264985
C	-2.43434	1.519733	-0.024928
H	-1.93964	2.062737	-2.084482
C	-1.53331	1.917818	-1.090197
H	0.44265	2.391798	-1.662886
C	-0.22138	2.098107	-0.857984
N	-4.77895	1.660445	-2.622516
N	-5.36873	0.587048	1.628205
C	2.25375	1.824747	1.978003
C	2.58277	2.413411	-0.359626
C	1.68242	2.048065	0.688143
C	0.33891	1.891972	0.462449
H	-0.15724	1.343921	2.520663
C	-0.56308	1.502009	1.528429
H	-2.53757	1.028620	2.102798
C	-1.87686	1.329702	1.298824
N	2.70191	1.618195	3.025184
N	3.29010	2.709813	-1.226283
H	-0.30949	-1.291692	-2.181225
C	-1.22848	-1.505645	-1.650085
H	-2.40487	-1.320037	-3.416938
C	-2.40797	-1.516157	-2.349903
C	-3.63040	-1.774879	-1.691677
H	-4.57375	-2.175445	0.183164
C	-3.63992	-1.994574	-0.339906
C	-1.19499	-1.755995	-0.251409
C	-2.43677	-1.976713	0.412582
H	-3.41487	-2.318564	2.308613
C	-2.45932	-2.166539	1.816370
H	-1.30579	-2.333295	3.605171
C	-1.29073	-2.170762	2.532632
H	0.85379	-2.058846	2.459461
C	-0.05866	-1.994626	1.877320
C	0.01998	-1.778221	0.513552
H	1.36422	-1.819476	-1.203254
C	1.32159	-1.597396	-0.142686
H	2.40538	-0.930071	1.524332
C	2.43947	-1.179968	0.467267
H	4.64731	-0.215224	1.651203
C	4.79714	-0.458181	0.604020
C	3.75083	-0.981157	-0.159817
H	3.27498	-1.673730	-2.162734
C	4.02880	-1.261220	-1.501839

Npe:TCNQ conformer b

SCF=-1388.26917485 E_h

0 1

H	4.62585	3.389692	-1.826617
N	-5.75810	0.986529	0.641421
H	-6.06930	0.085057	2.465172
C	-5.31518	0.492087	1.797268
H	-5.21563	1.883435	-1.132519
C	-4.84289	1.484443	-0.193042
C	3.96126	-1.339672	-1.040709
C	3.33787	-2.726725	0.854202
C	2.92248	-1.918669	-0.249337
C	1.59572	-1.726564	-0.537189
H	1.94589	-0.408492	-2.246386
C	1.18254	-0.904516	-1.657838
H	-0.41054	-0.133139	-2.805826
C	-0.11818	-0.748576	-1.962477
N	4.79778	-0.875301	-1.692091
N	3.65458	-3.385330	1.751741
C	-3.51024	-1.887661	-0.742907
C	-2.89597	-0.432566	-2.599359
C	-2.48204	-1.243342	-1.497863
C	-1.15614	-1.392463	-1.179516
H	-1.50881	-2.676963	0.553185
C	-0.74348	-2.198846	-0.047286
H	0.85197	-2.960579	1.106191
C	0.55740	-2.353731	0.257790
N	-4.31847	-2.431550	-0.118330
N	-3.20021	0.241862	-3.489559
H	0.48228	2.803311	-0.947693
C	1.51819	2.587000	-0.719241
H	2.21927	3.815694	-2.309945
C	2.49639	3.167541	-1.485021
C	3.86129	2.934836	-1.206340
H	5.25641	1.947413	0.073097
C	4.21178	2.136533	-0.151903
C	1.84443	1.732759	0.367830
C	3.22292	1.525243	0.661099
H	4.64582	0.550387	1.962864
C	3.59132	0.701189	1.753023
H	2.91927	-0.540081	3.354805
C	2.63283	0.100602	2.528026
H	0.53509	-0.253754	2.817912
C	1.27188	0.276349	2.224957
C	0.85420	1.072597	1.173205
H	-0.79517	1.518496	-0.166051
C	-0.56751	1.199261	0.844279
H	-1.40418	0.626125	2.686653
C	-1.59679	0.928853	1.660503
H	-3.68121	0.051234	3.119150
C	-3.97513	0.474046	2.163693
C	-3.01354	0.985110	1.288822
H	-2.80861	1.946176	-0.650528
C	-3.48166	1.508636	0.077710

Npe:TCNQ conformer c

SCF=-1388.27262371 E_h

0 1

C	-1.71706	-2.872065	1.930820
C	-3.81413	-1.682959	1.590617
C	-2.39322	-1.628375	1.733655
C	-1.70780	-0.444456	1.659809
H	0.26185	-1.333927	1.990844
C	-0.26397	-0.408786	1.787192
H	1.50220	0.740190	1.691564
C	0.42047	0.735636	1.622589
N	-1.14656	-3.866894	2.086551
N	-4.96510	-1.706228	1.471926
C	-0.22852	4.328498	0.659245
C	1.86416	3.128415	0.971888
C	0.43617	3.116077	1.018018
C	-0.26514	1.973900	1.308505
H	-2.24077	2.882685	1.073678
C	-1.71542	1.955701	1.269606
H	-3.48016	0.803118	1.366108
C	-2.39858	0.809573	1.430730
N	-0.78883	5.294060	0.352984
N	3.01994	3.111285	0.908024
H	0.30338	1.498617	-1.850985
C	-0.74234	1.220720	-1.894723
H	-1.36662	3.234764	-2.210458
C	-1.68084	2.202552	-2.094110
C	-3.05444	1.880757	-2.143481
H	-4.50601	0.315648	-2.032009
C	-3.45299	0.578468	-1.996637
C	-1.11744	-0.139652	-1.744384
C	-2.50500	-0.459331	-1.800044
H	-3.98156	-2.035056	-1.695380
C	-2.92142	-1.806189	-1.653244
H	-2.31555	-3.831212	-1.356759
C	-1.99814	-2.799088	-1.460052
H	0.08689	-3.295233	-1.259001
C	-0.62508	-2.488911	-1.394688
C	-0.16716	-1.193189	-1.515724
H	1.64303	-0.037187	-1.948587
C	1.26550	-0.887019	-1.388438
H	1.75758	-2.432295	-0.058565
C	2.11953	-1.571218	-0.617228
H	4.06842	-3.261062	0.190320
C	4.42373	-2.252964	0.000956
C	3.54287	-1.259083	-0.433733
H	3.45306	0.853209	-0.925170
C	4.07823	0.016040	-0.637268
H	5.85789	1.215255	-0.561100
C	5.43366	0.224995	-0.421044
H	-3.78734	2.665473	-2.298167
H	6.46416	-2.709469	0.508022
C	5.76629	-1.943532	0.179780
N	6.27888	-0.729453	-0.024632

Npe:TCNQ conformer d

SCF=-1388.27712288 E_h

0 1

C	1.96437	2.939945	-1.168401
C	0.17804	4.286118	-0.218664
C	0.57747	3.070416	-0.854071
C	-0.31842	2.063033	-1.105012
H	1.15143	0.675985	-1.946602
C	0.10562	0.807260	-1.694921
H	-0.43855	-1.130881	-2.326495
C	-0.77115	-0.189572	-1.904325
N	3.08807	2.811289	-1.414769
N	-0.16193	5.257314	0.311373
C	-4.45706	-0.907976	-1.472802
C	-2.65959	-2.314896	-2.307078
C	-3.06789	-1.050912	-1.778920
C	-2.17432	-0.035615	-1.568325
H	-3.64551	1.352716	-0.740485
C	-2.60056	1.227727	-0.999144
H	-2.04928	3.151568	-0.331509
C	-1.72153	2.218652	-0.774226
N	-5.58079	-0.777173	-1.229822
N	-2.31551	-3.335215	-2.730962
H	-0.24142	-2.692188	0.741179
C	-1.10901	-2.169480	1.125063
H	-2.41143	-3.793258	0.673716
C	-2.33169	-2.790475	1.080042
C	-3.48908	-2.127005	1.543040
H	-4.27821	-0.329417	2.382424
C	-3.39178	-0.852534	2.036297
C	-0.96860	-0.857248	1.648350
C	-2.14085	-0.187074	2.103293
H	-2.94271	1.634385	2.948982
C	-2.04199	1.136587	2.602598
H	-0.75434	2.782160	3.038376
C	-0.83053	1.771876	2.650095
H	1.29345	1.607460	2.313795
C	0.33603	1.106216	2.218046
C	0.29574	-0.179438	1.720274
H	1.55467	-1.935676	1.421827
C	1.52656	-0.858383	1.291690
H	2.55909	0.820235	0.571424
C	2.59312	-0.249917	0.756677
H	4.54121	0.804155	-0.776433
C	4.74612	-0.214609	-0.463648
C	3.83934	-0.907570	0.342644
H	3.54868	-2.805430	1.355719
C	4.18461	-2.213399	0.707120
H	5.65878	-3.765164	0.521818
C	5.37691	-2.752263	0.246120
H	-4.45310	-2.621660	1.494186
H	6.62749	-0.319980	-1.501202
C	5.91560	-0.846719	-0.871128
N	6.23974	-2.094998	-0.533651

2.4.3 Npe:TCNB Optimized Geometries

Npe:TCNB conformer a

E=1310.652160 E_h

0 1

N	-4.19737	-2.835595	-1.486689
C	-3.42182	-1.978913	-1.493854
N	-0.18609	-3.555226	-1.909517
C	-0.60947	-2.483960	-1.816092
N	1.07715	3.136304	-1.612539
C	0.28239	2.297536	-1.590540
N	-2.94264	3.874952	-1.063350
C	-2.52576	2.805567	-1.198513
H	-3.98887	0.593542	-1.201778
H	0.84996	-0.272665	-1.844503
C	-0.66588	1.222636	-1.564000
C	-2.03544	1.469537	-1.372963
C	-2.93321	0.405584	-1.351785
C	-2.47898	-0.898904	-1.513803
C	-1.10609	-1.144895	-1.689107
C	-0.20862	-0.082634	-1.719885
H	2.36241	1.572161	0.224087
H	1.83000	-1.028540	1.738304
H	6.59010	0.756996	-1.638932
H	6.15930	-2.390665	0.969763
N	6.47895	-0.858957	-0.368842
H	4.34539	1.649277	-1.074932
C	5.96505	0.243938	-0.912714
H	3.91639	-1.646458	1.663491
C	5.72414	-1.497169	0.529912
C	4.70701	0.743985	-0.596979
C	4.45806	-1.080182	0.914299
C	3.91417	0.071970	0.336814
C	2.57874	0.595022	0.648710
C	1.62943	-0.032120	1.356994
H	-4.04906	-2.551977	1.947560
H	-1.82827	-3.579436	1.490948
H	0.16965	-2.198775	1.346538
C	-3.16556	-1.924947	1.899139
C	-1.90478	-2.507995	1.642203
H	1.01239	2.542203	1.760826
C	-0.78049	-1.726486	1.564829
C	-3.26662	-0.569699	2.069488
H	-3.21033	2.106556	2.317810
H	-1.21000	3.544825	2.145077
H	-4.23111	-0.109906	2.264897
C	0.14262	1.896226	1.803145
C	0.30328	0.534395	1.643536
C	-0.84649	-0.318394	1.742979
C	-2.12167	0.265921	1.992918
C	-2.23249	1.671929	2.133728
C	-1.12280	2.469138	2.037773

Npe:TCNB conformer b

E=1310.651819 E_h

0 1

H	-2.87818	-2.205387	0.953701
H	-1.77413	0.588261	0.426267
N	1.82302	4.367473	-0.216614
C	1.83731	3.263360	-0.557493
N	-1.50894	2.532258	-1.748295
C	-0.48962	1.993062	-1.669064
N	5.28237	-1.497471	-0.767701
C	4.30735	-0.914794	-0.981021
N	2.03043	-3.243939	-2.579756
C	2.01986	-2.145744	-2.220159
H	3.91682	1.628642	-0.361884
H	-0.06893	-0.521395	-2.382534
C	0.74809	1.280220	-1.546743
C	1.87897	1.894332	-0.981257
C	3.05080	1.164425	-0.815398
C	3.10457	-0.169566	-1.211167
C	1.98168	-0.776924	-1.795614
C	0.80617	-0.048315	-1.955009
H	-7.49605	-1.413898	0.409416
H	-5.80916	1.973431	-1.198964
N	-6.76130	0.322467	-0.416799
H	-5.27970	-2.327062	1.038062
C	-6.59190	-0.851331	0.191298
H	-3.53102	1.223753	-0.670030
C	-5.65782	1.022563	-0.695176
C	-5.34868	-1.363552	0.542779
C	-4.37207	0.600806	-0.387302
C	-4.19584	-0.626899	0.260748
C	-2.88305	-1.163106	0.642191
C	-1.73789	-0.469154	0.667489
H	3.41129	1.979236	3.194207
H	1.14813	2.940654	2.802745
H	-0.62894	1.577393	1.844424
C	2.63224	1.363496	2.756936
C	1.34800	1.908488	2.536240
H	-0.84705	-2.946701	0.168168
C	0.35300	1.141755	1.984859
C	2.88381	0.055741	2.432421
H	3.12361	-2.522550	1.713067
H	1.36709	-3.911830	0.668397
H	3.86292	-0.379275	2.610980
C	-0.10880	-2.335305	0.676059
C	-0.41923	-1.028852	0.997315
C	0.58570	-0.208822	1.611629
C	1.87507	-0.762023	1.860287
C	2.13609	-2.114062	1.522104
C	1.16020	-2.884599	0.947736

Npe:TCNB conformer c

E=1310.649880 E_h

0 1

H	2.43359	2.055117	0.490868
H	2.12211	-0.911518	1.152582
N	-5.54502	-0.304294	0.650060
C	-4.52013	-0.608984	0.211457
N	-4.26690	0.987685	-3.037543
C	-3.61261	0.322062	-2.356088
N	0.37379	-3.632404	1.506409
C	-0.30327	-2.971002	0.843206
N	1.70868	-2.207356	-2.027817
C	0.63846	-1.967668	-1.663239
H	-2.76471	-2.165420	1.437096
H	-1.15312	-0.473747	-2.937129
C	-2.78297	-0.514771	-1.539428
C	-3.23388	-0.987144	-0.296101
C	-2.41737	-1.807910	0.476717
C	-1.14514	-2.145121	0.027869
C	-0.68581	-1.659188	-1.208670
C	-1.50828	-0.851389	-1.986750
H	7.11737	2.093539	-0.305781
H	6.06918	-1.817132	-1.022037
N	6.70641	0.111893	-0.684349
H	4.81267	2.677518	0.397193
C	6.33921	1.334601	-0.298914
H	3.72157	-1.414039	-0.383574
C	5.75987	-0.830044	-0.689107
C	5.04751	1.661970	0.093921
C	4.44202	-0.607547	-0.312700
C	4.06302	0.670786	0.106897
C	2.69757	1.001237	0.535513
C	1.80899	0.121684	1.013099
H	-3.03535	3.549681	-1.129261
H	-0.81076	3.063991	-2.137196
H	0.79345	1.636561	-0.973567
C	-2.32588	2.925806	-0.596869
C	-1.06276	2.650610	-1.165955
H	0.68684	-0.840205	3.165308
C	-0.15918	1.854630	-0.509135
C	-2.65890	2.378077	0.613140
H	-3.10631	1.147790	2.948756
H	-1.55048	-0.384045	4.117309
H	-3.63567	2.561663	1.050336
C	0.01391	-0.167392	2.643105
C	0.44241	0.428914	1.473885
C	-0.46002	1.287471	0.759271
C	-1.74921	1.543601	1.314428
C	-2.12274	0.937053	2.539874
C	-1.26131	0.088255	3.184203

Npe:TCNB conformer d

E=1310.648214 E_h

0 1

N	0.22911	3.953242	0.125114
C	-0.36723	3.047025	-0.273663
N	-3.83041	3.676900	0.513116
C	-3.21829	2.844039	-0.003771
N	-3.67218	-2.482557	-2.487241
C	-3.10091	-1.543445	-2.130705
N	0.38564	-2.250698	-2.727678
C	-0.24421	-1.370444	-2.322601
H	0.73070	0.923290	-1.416397
H	-4.20396	0.584523	-0.988557
C	-2.40700	-0.372813	-1.678422
C	-1.00944	-0.280740	-1.791490
C	-0.34812	0.857536	-1.340505
C	-1.07047	1.896811	-0.763103
C	-2.46788	1.798413	-0.635460
C	-3.13016	0.667638	-1.101173
H	0.18853	-2.564153	0.675098
H	0.84800	0.160683	1.886372
H	-4.49379	-2.624939	0.991475
H	-3.53772	0.892717	2.898044
N	-4.13282	-0.836611	1.948601
H	-2.11194	-3.160699	0.590783
C	-3.71810	-1.947087	1.337565
H	-1.12487	0.517423	2.605748
C	-3.18595	-0.001108	2.389341
C	-2.37954	-2.248919	1.115623
C	-1.82606	-0.213132	2.218183
C	-1.38894	-1.359751	1.542305
C	0.01209	-1.629900	1.203043
C	1.03860	-0.792233	1.402112
H	5.50593	2.938627	-0.820779
H	3.20983	3.429081	0.034363
H	1.80149	1.646764	0.869916
C	4.88180	2.131537	-0.452132
C	3.58326	2.410284	0.029208
H	2.32914	-3.140956	1.318614
C	2.78607	1.397014	0.496120
C	5.34755	0.843591	-0.447367
H	6.02528	-1.754454	-0.344781
H	4.60658	-3.602599	0.478629
H	6.34478	0.617734	-0.813150
C	2.93254	-2.320355	0.945657
C	2.41698	-1.041548	0.962419
C	3.23336	0.048935	0.510727
C	4.54437	-0.225267	0.028194
C	5.02241	-1.559789	0.022801
C	4.23440	-2.583787	0.475633

Npe:TCNB conformer e

E=1310.648088 E_h

0 1

H	-3.41825	2.604684	-0.410592
H	-1.28625	2.855747	0.470619
N	4.73265	-1.688165	1.720057
C	4.12367	-0.999329	1.019765
N	3.77916	-2.789370	-2.110603
C	3.42383	-1.788672	-1.654638
N	1.27785	4.158862	0.889016
C	1.64821	3.158575	0.443904
N	0.13539	2.950663	-2.831288
C	0.85186	2.317476	-2.182080
H	3.18801	1.387190	1.683792
H	1.87532	-0.023502	-2.885214
C	2.98109	-0.535162	-1.117469
C	3.34419	-0.137435	0.180546
C	2.91368	1.086778	0.681016
C	2.10574	1.911624	-0.095480
C	1.72701	1.506948	-1.386665
C	2.17267	0.290094	-1.892928
H	-6.20904	-0.988816	-1.849055
H	-4.56756	-2.349302	1.665748
N	-5.44771	-1.769799	-0.102855
H	-4.81465	1.061644	-1.812009
C	-5.50204	-0.822983	-1.040264
H	-3.09750	-0.372640	1.861232
C	-4.59155	-1.575779	0.902658
C	-4.72018	0.325644	-1.019647
C	-3.76178	-0.467879	1.011132
C	-3.80625	0.515029	0.019436
C	-2.96278	1.722729	0.033641
C	-1.71802	1.857588	0.507534
H	0.52147	-3.729570	-1.316862
H	-0.90290	-2.064826	-2.505060
H	-1.53089	0.033215	-1.412690
C	0.24168	-2.806110	-0.821623
C	-0.56279	-1.859661	-1.495233
H	-0.56776	2.003895	2.864960
C	-0.91924	-0.685831	-0.882883
C	0.67996	-2.545948	0.449748
H	1.43804	-1.788426	2.911530
H	0.87414	0.351136	4.018244
H	1.31099	-3.259521	0.971377
C	-0.32399	1.069992	2.367950
C	-0.84724	0.823681	1.116227
C	-0.49701	-0.390915	0.440231
C	0.33028	-1.338790	1.109877
C	0.81082	-1.055290	2.413389
C	0.49906	0.130918	3.024137

Npe:TCNB conformer f

E=1310.645596 E_h

0 1

H	0.79238	-0.458958	2.112141
H	0.59751	2.175850	0.572725
N	-3.78440	3.093156	-1.733286
C	-3.23200	2.082264	-1.641701
N	0.19163	2.777832	-2.538019
C	-0.43414	1.858024	-2.224647
N	-3.93412	-3.514447	0.068938
C	-3.33957	-2.620755	-0.359174
N	0.04417	-3.825343	-0.785247
C	-0.54485	-2.847599	-0.966511
H	-4.31311	-0.190936	-0.798734
H	0.52134	-0.588452	-1.855436
C	-1.18783	0.712814	-1.805460
C	-2.55694	0.824231	-1.509200
C	-3.26431	-0.283952	-1.051602
C	-2.61125	-1.499489	-0.876856
C	-1.24207	-1.612306	-1.177145
C	-0.53787	-0.506915	-1.643899
H	-3.78782	-1.332522	2.823376
H	-3.79785	2.610254	1.648439
N	-3.91393	0.637105	2.231966
H	-1.32919	-1.491983	2.579974
C	-3.21524	-0.468628	2.496256
H	-1.35597	2.637017	1.352174
C	-3.21940	1.711035	1.842821
C	-1.83536	-0.557465	2.357492
C	-1.84278	1.721319	1.668792
C	-1.11134	0.551986	1.909360
C	0.33283	0.423399	1.677802
C	1.07435	1.276895	0.958776
H	5.20371	-3.302330	-0.468673
H	2.72638	-3.385255	-0.150007
H	1.48748	-1.371272	0.379659
C	4.65534	-2.393880	-0.243255
C	3.25706	-2.443855	-0.053087
H	2.67688	3.304517	0.777552
C	2.55698	-1.303223	0.244851
C	5.30757	-1.193313	-0.159007
H	6.35620	1.263598	-0.020422
H	5.11464	3.367678	0.371822
H	6.37946	-1.136309	-0.323707
C	3.21020	2.374547	0.605100
C	2.50925	1.186037	0.646739
C	3.20015	-0.041706	0.363253
C	4.60549	0.006572	0.126733
C	5.28477	1.250315	0.154761
C	4.59841	2.413812	0.373584

3 Crystal data and structure

Table S13: Crystal data and structure refinement for CY_D1 (Npe:TCNB).

Identification code	CY_D1
Empirical formula	C27H15N5
Formula weight	409.44
Temperature/K	99.95(10)
Crystal system	monoclinic
Space group	P21/c
a/Å	6.7312(3)
b/Å	36.6599(13)
c/Å	9.5150(4)
α/°	90
β/°	106.283(4)
γ/°	90
Volume/Å^3	2253.79(17)
Z	4
ρ_{calc}g/cm^3	1.207
μ/mm^{-1}	0.586
F(000)	848.0
Crystal size/mm^3	0.17 × 0.077 × 0.037
Radiation	Cu Kα (λ = 1.54184)
2θ range for data collection/°	9.65 to 144.258
Index ranges	$-8 \leq h \leq 6, -44 \leq k \leq 39, -11 \leq l \leq 11$
Reflections collected	8966
Independent reflections	4325 [R_{int} = 0.0264, R_{sigma} = 0.0314]
Data/restraints/parameters	4325/102/353
Goodness-of-fit on F^2	1.085
Final R indexes [I>=2σ (I)]	R_1 = 0.1237, wR_2 = 0.3330
Final R indexes [all data]	R_1 = 0.1331, wR_2 = 0.3397
Largest diff. peak/hole / e Å^{-3}	0.94/-0.34

Table S14: Fractional Atomic Coordinates ($\times 10^4$) and Equivalent Isotropic Displacement Parameters ($Å^2 \times 10^3$) for CY_D1. U_{eq} is defined as 1/3 of the trace of the orthogonalised U_{IJ} tensor.

Atom	x	y	x	U (eq)
N2	-1655(7)	3894.2(11)	6917(4)	41.4(10)
N3	-1692(5)	2800.7(10)	6873(4)	29.1(8)
N4	-4799(5)	2831.7(10)	-677(4)	27.7(8)
N5	-4820(8)	3928.5(11)	-541(4)	46.0(11)
C18	-2127(7)	3733.5(11)	5830(5)	30.2(9)
C19	-2154(6)	2957.0(10)	5783(4)	21.2(8)
C20	-2705(6)	3538.1(11)	4466(4)	23.6(8)
C21	-2719(5)	3158.1(10)	4430(4)	19.3(8)
C22	-3270(5)	2974.0(10)	3104(4)	19.4(8)
C23	-3793(5)	3169.1(11)	1802(4)	20.7(8)
C24	-4354(6)	2981.1(11)	428(4)	21.3(8)
C25	-4372(7)	3759.5(12)	508(4)	31.4(10)
C26	-3787(6)	3552.2(11)	1842(4)	23.3(8)
C27	-3236(7)	3738.6(11)	3164(4)	27.5(9)
C7	2421(9)	4079.6(14)	4804(5)	44.1(12)
C8	2322(6)	3689.5(12)	4587(4)	28.1(9)
C9	2838(6)	3459.6(14)	5803(5)	33.5(10)
C10	2779(6)	3081.6(13)	5647(5)	31.3(10)
C11	2208(6)	2925.3(12)	4300(5)	28.5(9)
C12	1697(6)	3144.5(11)	3034(4)	24.1(8)
C13	1117(6)	2979.4(13)	1631(5)	31.5(10)
C14	613(7)	3184.4(15)	394(5)	37.1(11)
C15	658(7)	3563.2(15)	497(5)	37.2(11)
C16	1207(7)	3737.8(13)	1836(4)	31.6(10)
C17	1750(6)	3532.3(12)	3153(4)	24.7(9)
N1	3690(20)	5411(3)	6736(13)	73(3)
C1	4550(30)	5176(3)	7748(14)	90(4)
C2	4460(30)	4801(3)	7532(13)	89(4)
C3	3468(19)	4644(3)	6169(11)	47(2)
C4	2350(40)	4911(8)	5190(40)	69(4)
C5	2430(30)	5265(5)	5560(20)	68(4)
C6	3409(19)	4254(3)	5976(12)	50(2)
N1A	2350(30)	5407(4)	6920(20)	74(4)
C1A	2170(40)	5150(4)	7880(20)	90(4)
C2A	2360(40)	4779(5)	7630(20)	88(4)
C3A	2480(30)	4644(4)	6358(17)	44(3)
C4A	2930(60)	4887(14)	5160(60)	69(5)
C5A	3180(50)	5252(9)	5380(40)	72(5)
C6A	2460(30)	4249(5)	6080(19)	43(3)

Table S15: Anisotropic Displacement Parameters ($Å^2 \times 10^3$) for CY_D1. The Anisotropic displacement factor exponent takes the form: $-2\pi 2[h^2 a^* 2U_{11} + 2hka^* b^* U_{12} + \ldots]$.

Atom	U_{11}	U_{22}	U_{33}	U_{23}	U_{13}	U_{12}
N2	57(3)	35(2)	28(2)	-6.8(16)	4.1(18)	4.2(18)
N3	31.9(19)	30.1(19)	22.3(17)	0.9(14)	2.8(14)	0.5(14)
N4	28.5(17)	34.1(19)	20.6(17)	-1.4(14)	7.0(13)	-0.6(14)
N5	69(3)	38(2)	28(2)	9.2(17)	7.5(19)	8(2)
C18	39(2)	24(2)	24(2)	1.9(17)	4.8(17)	3.0(17)
C19	21.7(18)	22.1(18)	20.7(19)	-0.2(15)	7.5(14)	-0.9(15)
C20	26(2)	27(2)	17.0(18)	-1.5(15)	4.4(15)	0.6(15)
C21	14.0(16)	26.0(19)	18.0(18)	0.0(14)	4.6(13)	-0.1(14)
C22	18.6(17)	19.9(18)	20.4(18)	-0.8(14)	6.6(14)	-1.2(14)
C23	16.1(17)	27(2)	18.5(18)	-1.4(15)	4.1(14)	0.8(14)
C24	16.9(17)	28.2(19)	18.6(18)	1.0(15)	4.9(14)	-0.1(14)
C25	46(3)	26(2)	21(2)	0.2(17)	8.3(18)	3.2(18)
C26	26(2)	27(2)	16.3(18)	1.5(15)	4.3(15)	2.9(15)
C27	39(2)	21.9(19)	20.5(19)	2.4(15)	6.3(17)	2.2(17)
C7	61(3)	35(3)	34(2)	3(2)	9(2)	1(2)
C8	25(2)	33(2)	26(2)	-3.9(17)	6.2(16)	-1.4(16)
C9	23(2)	57(3)	19.0(19)	-4.5(18)	4.2(16)	-1.6(19)
C10	21(2)	45(3)	27(2)	10.3(18)	5.3(16)	-0.3(18)
C11	19.4(19)	32(2)	36(2)	6.9(17)	10.4(16)	3.7(16)
C12	15.5(17)	32(2)	26(2)	1.9(16)	7.5(15)	-1.8(15)
C13	19.6(19)	39(2)	37(2)	-11.4(19)	10.3(17)	-5.8(17)
C14	23(2)	64(3)	24(2)	-11(2)	6.9(17)	-8(2)
C15	29(2)	64(3)	19(2)	5(2)	6.7(17)	2(2)
C16	37(2)	36(2)	22(2)	4.4(17)	8.3(17)	1.6(18)
C17	22.6(19)	33(2)	16.9(18)	-1.1(15)	2.6(15)	1.0(16)
N1	98(8)	34(4)	83(6)	-3(4)	17(6)	-2(6)
C1	162(10)	41(5)	59(5)	1(4)	16(6)	-7(6)
C2	163(10)	37(4)	57(5)	-5(4)	11(6)	-9(6)
C3	65(6)	41(4)	38(4)	-1(3)	18(4)	9(5)
C4	86(13)	39(5)	78(5)	3(4)	17(8)	12(8)
C5	87(12)	42(4)	76(6)	-2(4)	23(7)	16(7)
C6	65(6)	41(4)	40(4)	1(3)	11(5)	4(5)
N1A	89(10)	39(6)	80(8)	5(6)	-1(9)	-8(8)
C1A	162(11)	33(6)	57(7)	-6(5)	4(8)	1(7)
C2A	160(11)	36(6)	52(6)	-12(5)	3(8)	5(7)
C3A	58(7)	38(5)	40(5)	3(4)	22(5)	5(6)
C4A	91(14)	38(6)	78(6)	-1(5)	20(9)	14(9)
C5A	91(14)	41(6)	80(7)	-3(6)	17(9)	12(9)
C6A	59(7)	38(5)	34(5)	-1(4)	17(6)	5(6)

Table S16: Bond Lengths for CY_D1.

Atom	Atom	Length/Å	Atom	Atom	Length/Å
N2	C18	1.155(6)	C11	C12	1.408(6)
N3	C19	1.149(5)	C12	C13	1.417(6)
N4	C24	1.148(5)	C12	C17	1.426(6)
N5	C25	1.141(6)	C13	C14	1.357(7)
C18	C20	1.437(5)	C14	C15	1.392(7)
C19	C21	1.439(5)	C15	C16	1.381(6)
C20	C21	1.393(5)	C16	C17	1.419(5)
C20	C27	1.398(5)	N1	C1	1.300(16)
C21	C22	1.387(5)	N1	C5	1.31(2)
C22	C23	1.388(5)	C1	C2	1.390(15)
C23	C24	1.432(5)	C2	C3	1.404(15)
C23	C26	1.405(5)	C3	C4	1.41(3)
C25	C26	1.437(5)	C3	C6	1.440(14)
C26	C27	1.388(5)	C4	C5	1.34(3)
C7	C8	1.444(6)	N1A	C1A	1.34(3)
C7	C6	1.296(12)	N1A	C5A	1.80(4)
C7	C6A	1.358(17)	C1A	C2A	1.40(2)
C8	C9	1.394(6)	C2A	C3A	1.33(2)
C8	C17	1.431(5)	C3A	C4A	1.55(6)
C9	C10	1.393(7)	C3A	C6A	1.47(2)
C10	C11	1.358(6)	C4A	C5A	1.36(4)

Table S17: Bond Angles for CY_D1.

Atom	Atom	Atom	Angle/°	Atom	Atom	Atom	Angle/°
N2	C18	C20	179.1(5)	C11	C12	C17	120.4(4)
N3	C19	C21	179.0(4)	C13	C12	C17	119.7(4)
C21	C20	C18	121.2(3)	C14	C13	C12	121.1(4)
C21	C20	C27	120.4(3)	C13	C14	C15	119.8(4)
C27	C20	C18	118.4(4)	C16	C15	C14	121.5(4)
C20	C21	C19	119.5(3)	C15	C16	C17	120.3(4)
C22	C21	C19	120.0(3)	C12	C17	C8	118.1(4)
C22	C21	C20	120.5(3)	C16	C17	C8	124.2(4)
C21	C22	C23	119.8(3)	C16	C17	C12	117.7(4)
C22	C23	C24	120.2(3)	C1	N1	C5	113.9(12)
C22	C23	C26	119.6(3)	N1	C1	C2	123.7(12)
C26	C23	C24	120.2(3)	C1	C2	C3	122.1(11)
N4	C24	C23	179.7(5)	C2	C3	C4	110.6(17)
N5	C25	C26	179.0(5)	C2	C3	C6	120.8(9)
C23	C26	C25	120.5(3)	C4	C3	C6	127.8(17)
C27	C26	C23	121.0(3)	C5	C4	C3	121(2)
C27	C26	C25	118.5(4)	N1	C5	C4	125.9(16)
C26	C27	C20	118.8(4)	C7	C6	C3	126.1(9)
C6	C7	C8	127.2(7)	C1A	N1A	C5A	116.3(18)
C6A	C7	C8	124.8(9)	N1A	C1A	C2A	122(2)
C9	C8	C7	119.3(4)	C3A	C2A	C1A	123.8(19)
C9	C8	C17	119.0(4)	C2A	C3A	C4A	122(2)
C17	C8	C7	121.6(4)	C2A	C3A	C6A	122.2(15)
C10	C9	C8	121.4(4)	C6A	C3A	C4A	115(2)
C11	C10	C9	120.8(4)	C5A	C4A	C3A	120(4)
C10	C11	C12	120.2(4)	C4A	C5A	N1A	113(3)
C11	C12	C13	119.9(4)	C7	C6A	C3A	127.6(14)

Table S18: Torsion Angles for CY_D1.

A	B	C	D	Angle/°	A	B	C	D	Angle/°
C18	C20	C21	C19	0.3(6)	C13	C12	C17	C16	0.0(6)
C18	C20	C21	C22	-179.6(4)	C13	C14	C15	C16	0.0(7)
C18	C20	C27	C26	179.7(4)	C14	C15	C16	C17	0.2(7)
C19	C21	C22	C23	-179.3(3)	C15	C16	C17	C8	-179.5(4)
C20	C21	C22	C23	0.6(5)	C15	C16	C17	C12	-0.2(6)
C21	C20	C27	C26	0.4(6)	C17	C8	C9	C10	-0.9(6)
C21	C22	C23	C24	179.7(3)	C17	C12	C13	C14	0.1(6)
C21	C22	C23	C26	-0.9(5)	N1	C1	C2	C3	2(3)
C22	C23	C26	C25	-178.5(4)	C1	N1	C5	C4	-17(2)
C22	C23	C26	C27	0.9(6)	C1	C2	C3	C4	-9(2)
C23	C26	C27	C20	-0.7(6)	C1	C2	C3	C6	179.7(15)
C24	C23	C26	C25	1.0(6)	C2	C3	C4	C5	4(3)
C24	C23	C26	C27	-179.6(4)	C2	C3	C6	C7	174.8(13)
C25	C26	C27	C20	178.7(4)	C3	C4	C5	N1	9(3)
C27	C20	C21	C19	179.6(4)	C4	C3	C6	C7	6(2)
C27	C20	C21	C22	-0.3(6)	C5	N1	C1	C2	11(3)
C7	C8	C9	C10	-179.6(4)	C6	C7	C8	C9	18.3(10)
C7	C8	C17	C12	179.8(4)	C6	C7	C8	C17	-160.2(8)
C7	C8	C17	C16	-1.0(7)	C6	C3	C4	C5	174.4(14)
C8	C7	C6	C3	-179.4(9)	N1A	C1A	C2A	C3A	-9(4)
C8	C7	C6A	C3A	-177.4(13)	C1A	N1A	C5A	C4A	18(3)
C8	C9	C10	C11	-0.2(6)	C1A	C2A	C3A	C4A	15(4)
C9	C8	C17	C12	1.2(6)	C1A	C2A	C3A	C6A	-173(2)
C9	C8	C17	C16	-179.6(4)	C2A	C3A	C4A	C5A	-1(4)
C9	C10	C11	C12	1.0(6)	C2A	C3A	C6A	C7	175(2)
C10	C11	C12	C13	179.6(4)	C3A	C4A	C5A	N1A	-14(3)
C10	C11	C12	C17	-0.8(6)	C4A	C3A	C6A	C7	-13(3)
C11	C12	C13	C14	179.8(4)	C5A	N1A	C1A	C2A	-7(3)
C11	C12	C17	C8	-0.4(6)	C6A	C7	C8	C9	-17.9(12)
C11	C12	C17	C16	-179.6(4)	C6A	C7	C8	C17	163.5(10)
C12	C13	C14	C15	-0.2(6)	C6A	C3A	C4A	C5A	-173(2)
C13	C12	C17	C8	179.3(4)					

Table S19: Crystal data and structure refinement for CY_B8b (2Npe:3TCNQ).

Identification code	**CY_B8b**
Empirical formula	C35H19N6
Formula weight	537.57
Temperature/K	102(3)
Crystal system	triclinic
Space group	P-1
a/Å	9.8862(4)
b/Å	11.8127(5)
c/Å	12.3102(5)
α/°	93.827(3)
β/°	93.940(3)
γ/°	111.868(4)
Volume/Å^3	1324.40(9)
Z	2
ρ_{calc}g/cm^3	1.348
μ/mm^{-1}	0.660
F(000)	556.0
Crystal size/mm^3	0.421 × 0.186 × 0.044
Radiation	Cu Kα (λ = 1.54184)
2θ range for data collection/Å	7.234 to 146
Index ranges	$-9 \leq h \leq 12, -14 \leq k \leq 14, -15 \leq l \leq 15$
Reflections collected	14402
Independent reflections	5154 [R_{int} = 0.0235, R_{sigma} = 0.0209]
Data/restraints/parameters	5154/0/379
Goodness-of-fit on F^2	1.031
Final R indexes [I>=2σ (I)]	R_1 = 0.0372, wR_2 = 0.1021
Final R indexes [all data]	R_1 = 0.0431, wR_2 = 0.1073
Largest diff. peak/hole / eÅ^{-3}	0.27/-0.20

Table S20: Fractional Atomic Coordinates ($\times 10^4$) and Equivalent Isotropic Displacement Parameters ($Å^2 \times 10^3$) for CY_B8b. U_{eq} is defined as 1/3 of the trace of the orthogonalised U_{IJ} tensor.

Atom	x	y	z	U(eq)
N1	1754.8(11)	2813.2(9)	5140.8(8)	24.2(2)
C1	1194.4(13)	3679.2(11)	5065.0(10)	25.7(3)
C2	1780.3(13)	4703.0(11)	4502.8(10)	24.8(2)
C3	3050.3(12)	4888.3(10)	3985.9(9)	21.4(2)
C4	3636.5(12)	3981.6(10)	4055.1(9)	23.3(2)
C5	2962.3(12)	2987.9(10)	4627.5(9)	23.0(2)
C6	3680.7(12)	5984.6(10)	3414.4(9)	23.3(2)
C7	4986.0(12)	6354.3(10)	3015.3(9)	20.9(2)
C8	5605.1(12)	7426.0(10)	2399.7(9)	20.1(2)
C9	4924.5(13)	8255.1(10)	2302.6(9)	23.5(2)
C10	5399.9(13)	9208.0(10)	1622.9(10)	24.9(2)
C11	6557.8(13)	9338.1(10)	1026.7(9)	23.8(2)
C12	7325.6(12)	8546.7(10)	1121.9(9)	20.7(2)
C13	8543.0(13)	8690.5(10)	522.8(9)	24.5(2)
C14	9327.7(13)	7955.6(11)	630.6(10)	26.5(3)
C15	8917.3(13)	7039.1(10)	1358.3(9)	24.1(2)
C16	7728.9(12)	6856.3(10)	1935.0(9)	21.3(2)
C17	6877.6(12)	7591.7(9)	1833.5(9)	19.1(2)
N2	3622.3(12)	1340.6(10)	1897.2(9)	30.2(2)
N3	1605.0(11)	-1815.1(9)	3678.5(8)	26.7(2)
N4	-5149.5(12)	1092.3(10)	4599.2(9)	33.0(3)
N5	-2828.5(12)	4011.3(9)	2777.1(9)	30.5(2)
C18	2644.7(13)	781.7(11)	2346.1(9)	22.6(2)
C19	1483.1(12)	-967.5(10)	3351.9(9)	21.2(2)
C20	1417.4(12)	110.7(10)	2917.2(9)	20.0(2)
C21	300.0(12)	524.4(10)	3037.1(8)	19.0(2)
C22	-920.0(12)	-97.3(10)	3649.2(9)	18.9(2)
C23	-1954.6(12)	371.2(10)	3802.3(8)	19.0(2)
C24	-1880.4(12)	1493.5(10)	3351.5(8)	18.6(2)
C25	-691.2(12)	2083.7(10)	2705.4(9)	20.0(2)
C26	336.5(12)	1618.9(10)	2554.8(9)	20.3(2)
C27	-2902.5(12)	2000.7(10)	3524.0(9)	20.0(2)
C28	-4128.5(13)	1468.2(10)	4135.1(9)	23.2(2)
C29	-2839.5(12)	3119.6(10)	3092.3(9)	22.3(2)
N6	621.3(11)	4687.9(10)	1454.5(9)	31.0(2)
N7	2584.4(12)	7746.7(9)	-449.0(9)	30.1(2)
C30	1571.4(13)	5193.4(10)	960.2(9)	23.0(2)
C31	2662.4(12)	6888.3(10)	-115.6(9)	21.8(2)
C32	2743.4(12)	5821.9(10)	329.2(9)	20.1(2)
C33	3863.1(12)	5422.4(9)	170.7(8)	18.6(2)
C34	5001.9(12)	6044.2(10)	-506.9(9)	19.9(2)
C35	3924.9(12)	4367.0(9)	671.2(9)	19.8(2)

Table S21: Anisotropic Displacement Parameters ($Å^2 \times 10^3$) for CY_B8b. The anisotropic displacement factor exponent takes the form: $-2\pi 2[h^2a^*2U_{11}+2hka^*b^*U_{12}+\ldots].$]

Atom	U_{11}	U_{22}	U_{33}	U_{23}	U_{13}	U_{12}
N1	24.8(5)	24.2(5)	24.2(5)	4.3(4)	1.9(4)	9.9(4)
C1	24.8(6)	26.7(6)	27.9(6)	4.9(5)	7.3(5)	11.4(5)
C2	24.5(6)	24.2(6)	29.6(6)	4.8(5)	6.1(5)	12.6(5)
C3	19.6(5)	22.5(5)	21.8(5)	1.7(4)	0.6(4)	7.9(4)
C4	20.3(6)	23.7(6)	26.6(6)	2.4(4)	2.7(4)	9.2(5)
C5	22.1(6)	22.0(6)	26.1(5)	2.2(4)	0.1(4)	10.0(5)
C6	23.5(6)	22.9(6)	25.3(5)	3.8(4)	2.3(4)	10.7(5)
C7	22.0(6)	20.0(5)	21.4(5)	1.8(4)	0.8(4)	9.0(4)
C8	20.6(5)	17.8(5)	21.5(5)	0.2(4)	-0.7(4)	7.5(4)
C9	21.7(6)	21.1(5)	28.2(6)	1.0(4)	2.0(4)	9.1(4)
C10	26.5(6)	19.1(5)	31.7(6)	1.0(4)	-1.7(5)	12.7(5)
C11	27.8(6)	16.9(5)	25.6(5)	3.5(4)	-1.8(4)	7.8(4)
C12	21.5(5)	16.6(5)	21.9(5)	0.9(4)	-1.1(4)	5.4(4)
C13	24.2(6)	21.4(5)	24.6(5)	3.6(4)	1.8(4)	4.6(4)
C14	21.9(6)	28.0(6)	28.0(6)	-0.4(5)	4.4(5)	7.8(5)
C15	23.2(6)	23.4(6)	27.5(6)	-0.2(4)	0.3(4)	11.6(5)
C16	22.8(6)	18.3(5)	23.1(5)	1.6(4)	-0.4(4)	8.7(4)
C17	20.4(5)	15.8(5)	19.7(5)	0.5(4)	-0.5(4)	5.8(4)
N2	27.9(5)	34.9(6)	34.3(6)	12.1(4)	10.4(4)	16.8(5)
N3	23.7(5)	27.0(5)	34.0(5)	7.8(4)	6.1(4)	13.5(4)
N4	30.8(6)	35.3(6)	44.7(6)	19.4(5)	16.1(5)	21.4(5)
N5	36.0(6)	25.3(5)	35.4(6)	8.2(4)	5.2(5)	16.6(4)
C18	23.1(6)	26.7(6)	22.9(5)	4.8(4)	3.3(4)	14.4(5)
C19	16.6(5)	26.1(6)	22.8(5)	2.1(4)	4.0(4)	9.9(4)
C20	19.6(5)	21.5(5)	19.8(5)	2.2(4)	1.3(4)	8.9(4)
C21	18.5(5)	20.2(5)	17.6(5)	0.9(4)	0.0(4)	7.1(4)
C22	19.6(5)	17.4(5)	19.8(5)	3.7(4)	0.7(4)	7.2(4)
C23	18.7(5)	19.1(5)	18.8(5)	3.6(4)	1.9(4)	6.6(4)
C24	18.6(5)	19.4(5)	17.8(5)	1.8(4)	-0.8(4)	7.8(4)
C25	20.0(5)	20.1(5)	20.6(5)	5.3(4)	2.2(4)	7.7(4)
C26	18.9(5)	21.3(5)	21.0(5)	6.0(4)	3.7(4)	7.2(4)
C27	20.2(5)	20.7(5)	20.7(5)	4.2(4)	2.7(4)	9.1(4)
C28	24.7(6)	23.9(6)	27.9(6)	8.3(5)	4.6(5)	15.7(5)
C29	21.4(6)	23.6(6)	24.8(5)	3.3(4)	3.8(4)	11.6(5)
N6	26.3(5)	31.5(6)	39.5(6)	12.3(5)	8.2(5)	13.4(5)
N7	30.0(5)	24.2(5)	39.2(6)	6.8(4)	-0.2(4)	13.9(4)
C30	21.9(6)	21.8(5)	27.8(6)	4.0(4)	0.1(5)	11.2(5)
C31	18.3(5)	21.5(6)	26.2(5)	2.0(4)	0.0(4)	8.7(4)
C32	20.2(5)	17.7(5)	22.6(5)	2.5(4)	0.0(4)	7.8(4)
C33	19.2(5)	16.1(5)	19.6(5)	0.6(4)	-1.6(4)	6.3(4)
C34	21.5(6)	16.5(5)	21.0(5)	3.7(4)	-0.3(4)	6.7(4)
C35	19.7(5)	17.5(5)	21.2(5)	3.8(4)	0.9(4)	6.0(4)

Table S22: Bond Lengths for CY_B8b.

Atom	Atom	Length/Å	Atom	Atom	Length/Å
N1	C1	1.3380(15)	N4	C28	1.1496(15)
N1	C5	1.3433(15)	N5	C29	1.1431(15)
C1	C2	1.3865(16)	C18	C20	1.4388(15)
C2	C3	1.3974(15)	C19	C20	1.4354(15)
C3	C4	1.3994(15)	C20	C21	1.3769(15)
C3	C6	1.4632(16)	C21	C22	1.4494(15)
C4	C5	1.3823(16)	C21	C26	1.4477(14)
C6	C7	1.3391(16)	C22	C23	1.3499(15)
C7	C8	1.4719(15)	C23	C24	1.4499(14)
C8	C9	1.3862(15)	C24	C25	1.4467(14)
C8	C17	1.4360(15)	C24	C27	1.3743(15)
C9	C10	1.4049(16)	C25	C26	1.3402(15)
C10	C11	1.3683(16)	C27	C28	1.4322(15)
C11	C12	1.4123(15)	C27	C29	1.4389(15)
C12	C13	1.4170(16)	N6	C30	1.1482(16)
C12	C17	1.4315(15)	N7	C31	1.1454(15)
C13	C14	1.3697(17)	C30	C32	1.4342(15)
C14	C15	1.4111(17)	C31	C32	1.4333(15)
C15	C16	1.3701(16)	C32	C33	1.3758(15)
C16	C17	1.4224(15)	C33	C34	1.4483(15)
N2	C18	1.1498(16)	C33	C35	1.4463(14)
N3	C19	1.1470(15)	C34	C35[1]	1.3428(15)

[1] 1-X,1-Y,-Z.

Table S23: Bond Angles for CY_B8b.

Atom	Atom	Atom	Angle/Å	Atom	Atom	Atom	Angle/Å
C1	N1	C5	115.57(10)	C19	C20	C18	115.22(9)
N1	C1	C2	124.17(11)	C21	C20	C18	120.38(10)
C1	C2	C3	119.91(11)	C21	C20	C19	124.38(10)
C2	C3	C4	116.21(10)	C20	C21	C22	121.88(10)
C2	C3	C6	119.62(10)	C20	C21	C26	119.81(10)
C4	C3	C6	124.17(10)	C26	C21	C22	118.30(9)
C5	C4	C3	119.46(10)	C23	C22	C21	120.33(10)
N1	C5	C4	124.66(10)	C22	C23	C24	120.99(10)
C7	C6	C3	125.51(10)	C25	C24	C23	118.39(9)
C6	C7	C8	125.99(10)	C27	C24	C23	121.76(10)
C9	C8	C7	120.72(10)	C27	C24	C25	119.85(9)
C9	C8	C17	118.71(10)	C26	C25	C24	120.56(10)
C17	C8	C7	120.47(9)	C25	C26	C21	121.33(10)
C8	C9	C10	121.78(10)	C24	C27	C28	123.63(10)
C11	C10	C9	120.35(10)	C24	C27	C29	122.57(10)
C10	C11	C12	120.35(10)	C28	C27	C29	113.80(9)
C11	C12	C13	120.67(10)	N4	C28	C27	175.58(11)
C11	C12	C17	119.88(11)	N5	C29	C27	177.29(12)
C13	C12	C17	119.45(10)	N6	C30	C32	179.17(12)
C14	C13	C12	121.45(11)	N7	C31	C32	178.37(12)
C13	C14	C15	119.20(11)	C31	C32	C30	115.29(9)
C16	C15	C14	121.02(11)	C33	C32	C30	121.85(10)
C15	C16	C17	121.32(10)	C33	C32	C31	122.86(10)
C12	C17	C8	118.74(10)	C32	C33	C34	120.77(10)
C16	C17	C8	123.75(10)	C32	C33	C35	120.76(10)
C16	C17	C12	117.51(10)	C35	C33	C34	118.47(10)
N2	C18	C20	178.55(12)	C35[1]	C34	C33	120.24(10)
N3	C19	C20	176.44(11)	C34[1]	C35	C33	121.29(10)

[1] 1-X,1-Y,-Z.

Table S24: Torsion angles for CY_B8b.

A	B	C	D	Angle/Å	A	B	C	D	Angle/Å
N1	C1	C2	C3	-1.12(19)	C15	C16	C17	C8	178.69(10)
C1	N1	C5	C4	0.54(17)	C15	C16	C17	C12	-1.19(16)
C1	C2	C3	C4	1.48(17)	C17	C8	C9	C10	3.39(16)
C1	C2	C3	C6	-178.66(11)	C17	C12	C13	C14	-1.76(17)
C2	C3	C4	C5	-0.91(16)	C18	C20	C21	C22	-177.19(10)
C2	C3	C6	C7	170.55(11)	C18	C20	C21	C26	2.03(16)
C3	C4	C5	N1	-0.10(18)	C19	C20	C21	C22	1.39(17)
C3	C6	C7	C8	177.30(10)	C19	C20	C21	C26	-179.39(10)
C4	C3	C6	C7	-9.60(19)	C20	C21	C22	C23	176.29(10)
C5	N1	C1	C2	0.08(17)	C20	C21	C26	C25	-176.35(10)
C6	C3	C4	C5	179.23(11)	C21	C22	C23	C24	0.66(16)
C6	C7	C8	C9	8.48(18)	C22	C21	C26	C25	2.89(16)
C6	C7	C8	C17	-167.77(11)	C22	C23	C24	C25	1.73(15)
C7	C8	C9	C10	-172.92(10)	C22	C23	C24	C27	-178.23(10)
C7	C8	C17	C12	171.41(10)	C23	C24	C25	C26	-1.80(15)
C7	C8	C17	C16	-8.47(16)	C23	C24	C27	C28	-1.21(17)
C8	C9	C10	C11	0.39(18)	C23	C24	C27	C29	179.40(10)
C9	C8	C17	C12	-4.92(15)	C24	C25	C26	C21	-0.53(16)
C9	C8	C17	C16	175.21(10)	C25	C24	C27	C28	178.83(10)
C9	C10	C11	C12	-2.59(17)	C25	C24	C27	C29	-0.57(17)
C10	C11	C12	C13	-178.80(11)	C26	C21	C22	C23	-2.94(15)
C10	C11	C12	C17	0.92(17)	C27	C24	C25	C26	178.17(11)
C11	C12	C13	C14	177.97(11)	C30	C32	C33	C34	177.46(10)
C11	C12	C17	C8	2.84(16)	C30	C32	C33	C35	-2.14(16)
C11	C12	C17	C16	-177.28(10)	C31	C32	C33	C34	-2.74(17)
C12	C13	C14	C15	-0.28(17)	C31	C32	C33	C35	177.65(10)
C13	C12	C17	C8	-177.44(9)	C32	C33	C34	C35[1]	-178.83(10)
C13	C12	C17	C16	2.45(16)	C32	C33	C35	C34[1]	178.82(10)
C13	C14	C15	C16	1.61(17)	C34	C33	C35	C34[1]	-0.79(17)
C14	C15	C16	C17	-0.84(17)	C35	C33	C34	C35[1]	0.78(17)

[1] 1-X,1-Y,-Z.